Bound states in the continuum

Chia Wei Hsu[1], Bo Zhen[2,3]*, A. Douglas Stone[1], John D. Joannopoulos[2] and Marin Soljačić[2]*

Abstract | Bound states in the continuum (BICs) are waves that remain localized even though they coexist with a continuous spectrum of radiating waves that can carry energy away. Their very existence defies conventional wisdom. Although BICs were first proposed in quantum mechanics, they are a general wave phenomenon and have since been identified in electromagnetic waves, acoustic waves in air, water waves and elastic waves in solids. These states have been studied in a wide range of material systems, such as piezoelectric materials, dielectric photonic crystals, optical waveguides and fibres, quantum dots, graphene and topological insulators. In this Review, we describe recent developments in this field with an emphasis on the physical mechanisms that lead to BICs across seemingly very different materials and types of waves. We also discuss experimental realizations, existing applications and directions for future work.

The partial or complete confinement of waves is ubiquitous in nature and in wave-based technology. Examples include electrons bound to atoms and molecules, light confined in optical fibres and the partial confinement of sound in musical instruments. The allowed frequencies of oscillation are known as the wave spectrum.

To determine whether a wave can be perfectly confined or not (that is, if a 'bound state' exists or not) in an open system, a simple criterion is to look at its frequency. If the frequency is outside the continuous spectral range spanned by the propagating waves, it can exist as a bound state because there is no pathway for it to radiate away. Conversely, a wave state with the frequency inside the continuous spectrum can only be a 'resonance' that leaks and radiates out to infinity. This is the conventional wisdom described in many books. A bound state in the continuum (BIC) is an exception to this conventional wisdom: it lies inside the continuum and coexists with extended waves, but it remains perfectly confined without any radiation. BICs are found in a wide range of material systems through confinement mechanisms that are fundamentally different from those of conventional bound states.

The general picture is clear from the spectrum and the spatial profile of the modes (FIG. 1). More specifically, consider waves that oscillate in a sinusoidal way as $e^{-i\omega t}$ in time t and at angular frequency ω. Extended states (blue; FIG.1) exist across a continuous range of frequencies. Outside this continuum lie discrete levels of conventional bound states (green; FIG.1) that have no access to radiation channels; this is the case for the bound electrons of an atom (at negative energies), the guided modes of an optical fibre (below the light line) and the defect modes in a bandgap. Inside the continuum, resonances (orange; FIG.1) may be found that locally resemble a bound state but in fact couple to the extended waves and leak out; they can be associated with a complex frequency, $\omega = \omega_0 - i\gamma$, in which the real part ω_0 is the resonance frequency and the imaginary part γ represents the leakage rate. This complex frequency is defined rigorously as the eigenvalue of the wave equation with outgoing boundary conditions[1,2]. In addition to these familiar wave states, there is the less known possibility of BICs (red; FIG.1) that reside inside the continuum but remain perfectly localized with no leakage, namely $\gamma = 0$. In a scattering experiment, waves coming in from infinity can excite the resonances, causing a rapid variation in the phase and amplitude of the scattered waves within a spectral linewidth of 2γ. However, such waves cannot excite BICs, because BICs are completely decoupled from the radiating waves and are invisible in this sense. Therefore, a BIC can be considered as a resonance with zero leakage and zero linewidth ($\gamma = 0$; or infinite quality factor $Q = \omega_0/2\gamma$). BICs are sometimes referred to as embedded eigenvalues or embedded trapped modes.

In 1929, BICs were proposed by von Neumann and Wigner[3]. As an example, von Neumann and Wigner mathematically constructed a 3D potential extending to infinity and oscillating in a way that was tailored to support an electronic BIC. This type of BIC-supporting system is rather artificial and has never been realized. However, since this initial proposal, other mechanisms leading to BICs have been identified in different material

[1]*Department of Applied Physics, Yale University, New Haven, Connecticut 06520, USA.*
[2]*Research Laboratory of Electronics, Massachusetts Institute of Technology, Cambridge, Massachusetts 02139, USA.*
[3]*Physics Department and Solid State Institute, Technion, Haifa 32000, Israel.*
**These authors contributed equally to this work.*
Correspondence to C.W.H. and B.Z.
chiawei.hsu@yale.edu; bozhen@mit.edu

Article number: 16048
doi:10.1038/natrevmats.2016.48
Published online 19 Jul 2016

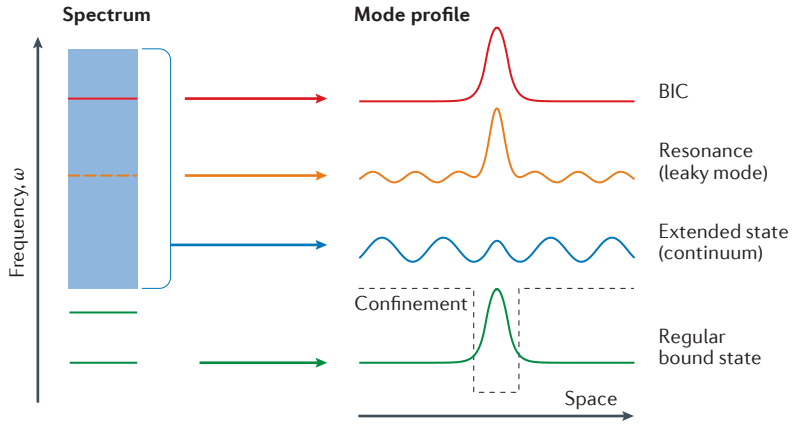

Figure 1 | **Illustration of a BIC.** In an open system, the frequency spectrum consists of a continuum or several continua of spatially extended states (blue) and discrete levels of bound states (green) that carry no outgoing flux. The spatial localization of the bound states is a consequence of a confining structure or potential (black dashed line). States inside the continuous spectrum typically couple to the extended waves and radiate, becoming leaky resonances (orange). Bound states in the continuum (BICs; red) are special states that lie inside the continuum but remain localized with no radiation.

systems, many of which have been observed in experiments in electromagnetic, acoustic and water waves. In recent years, photonic structures have emerged as a particularly attractive platform owing to the ability to tailor the material and structure, which is often impossible in quantum systems. The unique properties of BICs have led to numerous applications, including lasers, sensors, filters and low-loss fibres, with many more possible uses proposed and yet to be implemented.

Most theoretically proposed and all experimentally observed BICs are realized in extended structures because, in most wave systems, BICs are forbidden in compact structures (BOX 1). Among the extended structures that support BICs, many are uniform or periodic in one or more directions (for example, x and y), and the BIC is localized only in the other directions (for example, z). In such systems, the concept of BICs requires careful definition. More specifically, because translational symmetry conserves the wave vector, $\mathbf{k}_{//} = (k_x, k_y)$, a state is considered a BIC when it exists inside the continuous spectrum of modes at the same $\mathbf{k}_{//}$ but remains localized and does not radiate in the z direction. These BICs are typically found at isolated wave vectors.

In this Review, we present the concepts and physical mechanisms that unify BICs across various material systems and in different types of waves, focusing on experimental studies and applications. First, we describe BICs protected by symmetry and separability; second, we discuss BICs achieved through parameter tuning (with coupled resonances or with a single resonance); and third, we describe BICs built with inverse construction (for example, potential, hopping rate or shape engineering). We conclude with the existing and emerging applications of BICs.

Bound states due to symmetry or separability

The simplest places to find BICs are in systems in which the coupling of certain resonances to the radiation modes are forbidden by symmetry or separability.

Symmetry-protected BICs. When a system exhibits a reflection or rotational symmetry, modes of different symmetry classes completely decouple. It is common to find a bound state of one symmetry class embedded in the continuous spectrum of another symmetry class, and their coupling is forbidden as long as the symmetry is preserved.

The simplest example concerns sound waves in air, with a plate placed along the centreline of an acoustic waveguide (FIG. 2a). The fluctuation of air pressure, p, follows the scalar Helmholtz equation with Neumann boundary condition $\partial p/\partial n = 0$ on the surfaces of the walls and of the plate, where n is the direction normal to the surface. The waveguide supports a continuum of waves propagating in the x direction that are either even or odd under mirror reflection in the y direction; the odd modes (red; FIG. 2a, middle panel) require at least one oscillation in the y direction and only exist above a cut-off frequency, $\pi c_s/h$, where c_s is the speed of sound and h is the width of the waveguide. The plate respects the mirror symmetry and, as a result, modes localized near it are also even or odd in the y direction, and an odd mode below the cut off is guaranteed to be a bound state despite being embedded in the continuum of even extended modes (FIG. 2a). Parker first measured[4] and analysed[5] such modes using a cascade of parallel plates in a wind tunnel. These modes can be excited from the near field and are audible with a stethoscope placed near the plates. This plate-in-waveguide system has been studied by others[6–8], and obstacles with arbitrary symmetric shapes have also been considered[9]. It should be noted that obstacles that are infinitesimally thin and parallel to the waveguide are decoupled from the fundamental waveguide mode even without mirror-in-y symmetry[10–13].

Similar symmetry-protected bound states exist in canals as surface water waves[14–20], in quantum wires[21–23], or for electrons in potential surfaces with antisymmetric couplings[24]. A common setup is a 1D waveguide or lattice array that supports a continuum of even-in-y extended states, with two defects attached symmetrically above and below this array to create an odd-in-y defect bound state. This configuration has been explored with the defects comprising single-mode optical waveguides[25–28], mechanically coupled beads[29,30], quantum dots[31–41], graphene flakes[42,43], ring structures[37,44,45] or impurity atoms[46,47]. Experimental realizations are demonstrated in two of these studies[27,28], both using coupled optical waveguides. When the mirror symmetry is broken, the bound state turns into a leaky resonance. In one example, the mirror symmetry is broken by bending the defect waveguides, which allows coupling light into and out of the would-be BIC[27]. In another case, a temperature gradient changes the refractive index of the material and breaks the mirror symmetry, which induces radiation in a controllable manner[28] (FIG. 2b).

Symmetry-protected BICs also exist in periodic structures: for example, a photonic crystal (PhC) slab[48] comprising a square array of cylindrical holes etched into a dielectric material (FIG. 2c). Because of the periodicity in the x and y directions, the photonic modes can be labelled by $\mathbf{k}_{//} = (k_x, k_y)$. When the 180° rotational symmetry around the z axis (C_2) is preserved (for example,

at $\mathbf{k}_{//} = (0, 0)$, commonly known as the Γ point), even and odd modes with respect to C_2 are decoupled. At frequencies below the diffraction limit of $\omega_c = 2\pi c/na$ (where a is the periodicity, n is the refractive index of the surrounding medium and c is the vacuum speed of light), the only radiating states are plane waves in the normal direction (z) with the electric and magnetic field vectors being odd under C_2; therefore, any even mode at the Γ point is a BIC. Away from the Γ point, these states start to couple to radiation, because they are no longer protected by C_2. This disappearance of radiation has been observed in early experiments on periodic metallic grids[49], documented in theoretical studies on PhC slabs[50–56] and measured quantitatively from the Q of resonances in large-area PhC slabs[57] (FIG. 2c). The suppressed radiation has also been characterized in the lasing pattern of 1D periodic gratings[58,59]. Such photonic BICs are commonly realized in silicon photonics and with III–V semiconductors, and have found applications in lasers, sensors and filters (see the last section).

In crystal acoustics, symmetry-protected BICs exist as the surface acoustic wave (SAW) in anisotropic solids, such as piezoelectric materials. This phenomenon can be used to enhance performance beyond the typical limit of bulk materials. For example, the phase velocity, $V = \omega/|\mathbf{k}_{//}|$, of a SAW is limited to the speed of the slowest bulk wave, otherwise it becomes a leaky resonance. However, along high-symmetry directions, symmetry may decouple the SAW from the bulk waves, turning the resonance into a supersonic but perfectly confined SAW[60–64], allowing higher phase velocity than the bulk limit. A related example exists in optics in uniform slabs with anisotropic permittivity and permeability tensors[65].

Box 1 | **Non-existence of single-particle BICs in compact structures**

Most structures supporting bound states in the continuum (BICs) extend to infinity in at least one direction. This is because BICs are generally forbidden in compact structures for single-particle-like systems.

Consider a 3D compact optical structure in air, characterized by its permittivity $\varepsilon(\mathbf{r})$ and permeability $\mu(\mathbf{r})$, with R as the radius of a sphere that encloses the structure. Outside the bounding sphere $\varepsilon(\mathbf{r}) = \mu(\mathbf{r}) = 1$; therefore, the electric (**E**) and magnetic (**H**) fields follow the Helmholtz equation and can be expanded in spherical harmonics and spherical Hankel functions with wavenumber $k = \omega/c$. A bound state must have no radiating far field, but every term in the expansion carries an outgoing Poynting flux, and hence, all terms must be zero, meaning that **E** and **H** must both vanish for $|\mathbf{r}| > R$. If $\varepsilon(\mathbf{r})$ and $\mu(\mathbf{r})$ are neither infinite nor zero anywhere, continuity of the fields requires **E** and **H** to be zero everywhere in space, and as a result, such a bound state cannot exist[254]. The same argument applies to a 1D or 2D system.

This non-existence theorem does not exclude compact BICs when the material has $\varepsilon = \pm\infty$, $\mu = \pm\infty$, $\varepsilon = 0$ or $\mu = 0$, which can act as hard walls that spatially separate the bound state from the extended ones. Examples with $\varepsilon = 0$ have been proposed[251,254,255] but are difficult to realize because typically the loss $\mathrm{Im}(\varepsilon)$ is significant at the plasma frequency of a metal, where $\mathrm{Re}(\varepsilon) = 0$.

The same argument applies to the single-particle Schrödinger equation. For an electron with a non-vanishing effective mass (m; the $m = 0$ case is studied in REF. 256) in a compact and finite potential ($V(\mathbf{r}) = 0$ for $|\mathbf{r}| > R$, and $V(\mathbf{r}) \neq \pm\infty$ everywhere), a bound state with positive energy $E > 0$ cannot exist. Similarly, this non-existence theorem can be applied to acoustic waves in air and to linearized water waves in constant-depth (z-independent) structures, because both systems are described by the Helmholtz equation. However, this theorem does not apply to water waves in structures with z dependence[80], which follow the Laplace equation instead.

Separable BICs. Separability can also be exploited to construct BICs. For example, consider a 2D system with a Hamiltonian of the form

$$H = H_x(x) + H_y(y) \tag{1}$$

where H_x acts only on the x variable and H_y acts only on the y variable. It is possible to separately solve the 1D eigen-problems $H_x\Psi_x^{(n)}(x) = E_x^{(n)}\Psi_x^{(n)}(x)$ and $H_y\Psi_y^{(m)}(y) = E_y^{(m)}\Psi_y^{(m)}(y)$. If $\Psi_x^{(n)}(x)$ and $\Psi_y^{(m)}(y)$ are bound states of the 1D problems, their product wavefunction, $\Psi_x^{(n)}(x)\Psi_y^{(m)}(y)$, is bound in both dimensions and will remain localized even if its eigenvalue, $E_x^{(n)} + E_y^{(m)}$, lies within the continuous spectrum of the extended states for the 2D Hamiltonian; coupling to the extended states is forbidden by separability. This type of BIC was first proposed by Robnik[66], and subsequently studied in other quantum systems[67–69] and in Maxwell's equation in 2D[70–73]. So far, separable BICs have not been observed experimentally, but there are promising examples in several material systems, including photorefractive medium, optical traps for cold atoms and certain lattices described by tight-binding models[74].

Bound states through parameter tuning

When the number of radiation channels is small, tuning the parameters of the system may be enough to completely suppress radiation into all channels. Generally, if radiation is characterized by N degrees of freedom, at least N parameters need to be tuned to achieve a BIC. In many cases, this suppression can be interpreted as an interference effect in which two or more radiating components cancel each other. We describe three different scenarios in the following subsections.

Fabry–Pérot BICs (coupled resonances). A resonant structure coupled to a single radiation channel is known to cause unity reflection near the resonance frequency, ω_0, when there are no other losses. This is because the direct transmission and the resonant radiation interfere and completely cancel each other[75]. Two such resonant structures can act as a pair of perfect mirrors that trap waves in between them. BICs are formed when the resonance frequency or the spacing, d, between the two structures is tuned to make the round-trip phase shifts add up to an integer multiple of 2π (FIG. 3a). This structure is equivalent to a Fabry–Pérot cavity formed between two resonant reflectors.

Temporal coupled-mode theory[76] provides a simple tool to model such BICs. In the absence of external driving sources, the two resonance amplitudes $A = (A_1, A_2)^T$ evolve in time as $i\partial A/\partial t = HA$ with Hamiltonian[77–79]

$$H = \begin{pmatrix} \omega_0 & \kappa \\ \kappa & \omega_0 \end{pmatrix} - i\gamma \begin{pmatrix} 1 & e^{i\psi} \\ e^{i\psi} & 1 \end{pmatrix} \tag{2}$$

where κ is the near-field coupling between the two resonators, γ is the radiation rate of the individual resonances and $\psi = kd$ is the propagation phase shift between the two resonators, where k is the transverse wavenumber (FIG. 3a). The two eigenvalues of H are

$$\omega_\pm = \omega_0 \pm \kappa - i\gamma(1 \pm e^{i\psi}) \tag{3}$$

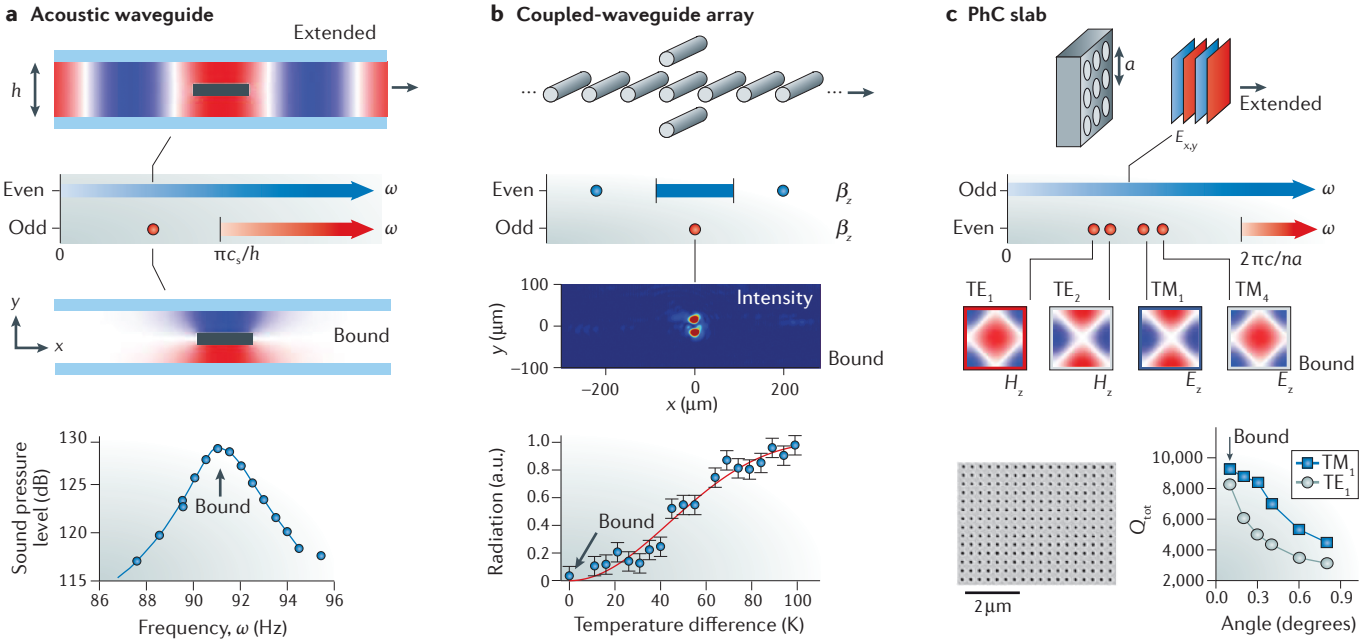

Figure 2 | **Symmetry-protected bound states. a** | An acoustic waveguide with an obstructing plate (black) placed at the centre. An odd bound state exists at the same frequency as an even extended state but cannot couple to it. Measuring the sound pressure near the plate reveals the bound state (bottom panel)[6]. **b** | A coupled-waveguide system with two defects placed symmetrically parallel to a linear array, which supports a similar odd bound state. The propagation constant, β_z, has the role of frequency. A temperature gradient can break the mirror symmetry by the thermo-optic effect and turn the bound state into a leaky resonance (bottom panel)[28]. **c** | A photonic crystal (PhC) slab with a 180° rotational symmetry around the *z* axis (C_2). At the Γ point, modes that are even under C_2 cannot radiate because plane waves in the normal direction are odd under C_2. Away from the normal direction, the bound states become leaky with finite quality factors (*Q*s), as confirmed by reflectivity measurements (bottom panel)[57]. $\pi c_s/h$, cut-off frequency (where c_s is the sound speed and *h* is the width of the waveguide); $2\pi c/na$, diffraction limit (where *c* is the vacuum speed of light, *n* is the refractive index of the surrounding medium and *a* is periodicity); a.u., arbitrary units; $E_{x,y,z}$, the *x*, *y* and *z* components of the electric field; *h*, height; H_z, the *z* component of the magnetic field; Q_{tot}, total quality factor; $TE_{1,2}$, first and second transverse-electric-like modes; $TM_{1,4}$, first and fourth transverse-magnetic-like modes; *ω*, angular frequency.

When ψ is an integer multiple of π (namely, when the round trip phase shift is an integer multiple of 2π), one of the two eigenmodes becomes more lossy with twice the original decay rate, and the other eigenmode becomes a BIC with a purely real eigenfrequency.

Fabry–Pérot BICs are commonly found in systems with two identical resonances coupled to a single radiation channel. They exist in water waves between two obstacles[80–85], as first proposed by McIver[80] — these are sometimes called sloshing trapped modes[86]. In quantum mechanics, they are found in impurity pairs in a waveguide[20,87], in time-dependent double-barrier structures[88], in quantum dot pairs connected to a wire[89–93], in double metal chains on a metal substrate[94] or in double waveguide bends[95]. In photonics, Fabry–Pérot BICs exist in structures ranging from stacked PhC slabs[96–98] and double gratings[99,100], to off-channel resonant defects connected to a waveguide or waveguide array[25,27,45,77,101,102]. Such BICs have also been studied in acoustic cavities[103]. A unique property of Fabry–Pérot BICs is that the two resonators interact strongly through radiation even when they are far apart. These long-range interactions have been studied in cavities or qubits coupled through a waveguide[104–106] and for two leaky solitons coupled through free-space radiation[107].

The same principle applies when a single resonant structure is next to a perfectly reflecting boundary, such as a hard wall, lattice termination or a PhC with a band-gap. For example, Fabry–Pérot BICs exist on the surface of a photonic crystal[108] and in a semi-infinite 1D lattice with a side-coupled defect, which has been predicted[109] and then experimentally realized[110] using coupled optical waveguides (FIG. 3b). This principle can be extended to polar or spherical coordinates[111,112].

Friedrich–Wintgen BICs (coupled resonances). The intuitive unity-reflection explanation of Fabry–Pérot BICs applies when the two resonators are far apart. However, equation 3 shows that a BIC can arise even with no separation ($d = 0$). In other words, two resonances at the same location can lead to a BIC through interference of radiation — unity reflection is not a requirement.

In temporal coupled-mode theory, when two resonances reside in the same cavity and are coupled to the same radiation channel, the resonance amplitudes evolve with the Hamiltonian[113,114]

$$H = \begin{pmatrix} \omega_1 & \kappa \\ \kappa & \omega_2 \end{pmatrix} - i \begin{pmatrix} \gamma_1 & \sqrt{\gamma_1\gamma_2} \\ \sqrt{\gamma_1\gamma_2} & \gamma_2 \end{pmatrix} \quad (4)$$

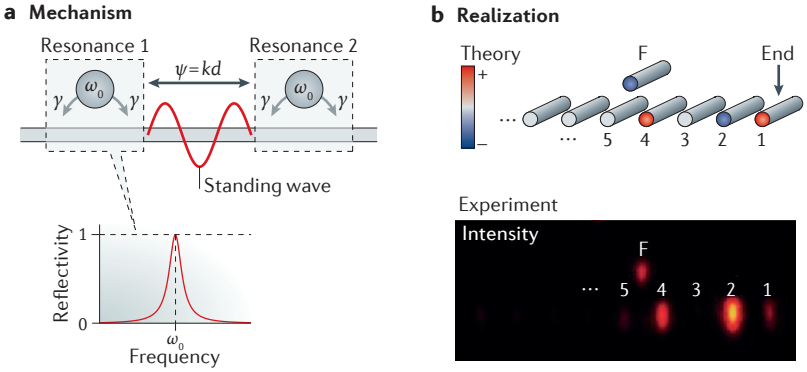

Figure 3 | **Fabry–Pérot BICs. a** | A schematic illustration of the Fabry–Pérot bound state in the continuum (BIC). Two identical resonances radiate into the same radiation channel, and each resonance acts as a perfect reflector at the resonance frequency, ω_0; therefore, waves can be trapped in between the two resonances when the round-trip phase shift is an integer multiple of 2π. **b** | Realization of a Fabry–Pérot BIC in a semi-infinite coupled waveguide array, in which the defect waveguide (F) and its mirror image with respect to the end are the two resonances. γ, radiation rate; $\psi = kd$, propagation phase shift between two resonators (where k is the transverse wavenumber and d is distance). Part **b** is adapted with permission from REF. 110, American Physical Society.

Here, we consider the scenario in which the two resonances can have different resonance frequencies, $\omega_{1,2}$, and different radiation rates, $\gamma_{1,2}$. The two resonances radiate into the same channel, and hence, interference of radiation gives rise to the via-the-continuum coupling term $\sqrt{\gamma_1\gamma_2}$. As a result, when

$$\kappa(\gamma_1 - \gamma_2) = \sqrt{\gamma_1\gamma_2}\,(\omega_1 - \omega_2) \quad (5)$$

one eigenvalue becomes purely real and turns into a BIC and the other eigenvalue becomes more lossy. This type of BIC is named after those who first derived equation 5 — Friedrich and Wintgen[115]. Note that when $\kappa = 0$ or when $\gamma_1 = \gamma_2$, the BIC is obtained at $\omega_1 = \omega_2$; therefore, when $\kappa \approx 0$ or $\gamma_1 \approx \gamma_2$, Friedrich–Wintgen BICs occur near the frequency crossings of the uncoupled resonances. Generally, these BICs are possible when the number of resonances exceeds the number of radiation channels[116,117], but the required number of tuning parameters also grows with the number of radiation channels.

The first examples of Friedrich–Wintgen BICs were proposed in atoms and molecules[118,119], and their effects have been observed experimentally as a suppressed autoionization in certain doubly excited Rydberg states of barium[120]. More recently, these BICs have been studied in continuum shell models[121], cold-atom collisions[122], 2D topological insulators with a defect[123], and for quantum graphs[124], quantum billiards[125] or impurity atoms[126,127] attached to waveguides. In acoustics, they have been studied in multiresonant cavities[103,128]. In optics, they have been studied in multiresonant dielectric objects in microwave waveguides[129,130] and as 'dark state lasers' (REF. 131).

Single-resonance parametric BICs. The preceding examples relate to two (or more) coupled resonances whose radiations cancel to produce BICs. Meanwhile, a single resonance can also evolve into a BIC when enough parameters are tuned. The physical picture is similar to the preceding examples; here, the single resonance itself can be thought of as arising from two (or more) sets of waves, and the radiation of the constituting waves can be tuned to cancel each other.

BICs tuned from a single resonance have been predicted and realized in a PhC slab[132], as shown in FIG. 4a. At wave vectors away from $\mathbf{k}_{//} = (0, 0)$, modes above the light line ($\omega > |\mathbf{k}_{//}|c/n$) radiate and form leaky resonances[54]. When the PhC slab has C_2 symmetry, up–down mirror symmetry and time-reversal symmetry, the number of radiation channels is reduced[132]. At a generic k point along the Γ-to-X direction, the resonance turns into a bound state, as shown by the diverging radiative quality factor, Q_r (FIG. 4a). Q_r can be determined through the reflectivity spectrum[132], or through the photocurrent spectrum by embedding a detector in the slab[133]. Such BICs also exist in a linear periodic array of rectangles[134,135], cylinders[136] or spheres[137], and related BICs have been found in time-periodic systems[138]. It is possible to analyse them through spatial coupled-wave theory[139]. With the mode expansion method, one can solve for the BICs efficiently and also reveal which sets of waves interfere to cancel the radiation[134,135,140]. Although these BICs are not guaranteed to exist by symmetry, when they do exist they are robust to small changes in the system parameters, and their generation, evolution and annihilation follow strict rules that can be understood through the concept of topological charges[141], which also governs other types of BICs (BOX 2). These BICs can be described as 'topologically protected' and are known to exist generically if the system parameters (for example, the lattice spacing and thickness of the PhC) can be varied over a sufficient range. The topological protection of BICs in a periodic structure has been studied in quantum Hall insulators[142] (BOX 2).

Single-resonance parametric BICs can also exist in non-periodic structures, as shown theoretically in acoustic and water waveguides with an obstacle[143–148], in quantum waveguides with impurities[149–151] or bends[95,152,153], for mechanically coupled beads[29,30] and mechanical resonators[154], and in optics for a low-index waveguide on a high-index membrane[155].

These types of BICs also manifest themselves through other types of SAWs in anisotropic solids. For example, it was predicted[156,157] that on the (001) plane of GaAs, the leaky SAWs become true surface waves (that is, no leakage into the bulk) at a propagation direction of $\phi \approx 33°$ (where ϕ is the angle from the [100] direction), in addition to the more well-known symmetry-protected SAW at the [110] direction of $\phi = 45°$ (FIG. 4b). The reduced attenuation near $\phi \approx 33°$ was observed experimentally[158,159]. Such SAWs exist in other solids[160–168] and are sometimes called secluded supersonic SAWs[161]. With a periodic mass loading on the surface, secluded supersonic SAWs may also be found in isotropic solids[169–171]. This type of acoustic BIC was first reported in a piezoelectric material, $LiNbO_3$ (REF. 172), and has been used in supersonic SAW devices[173–176] (see the last section).

Bound states from inverse construction

Instead of looking for the presence of BICs in a given system, the problem can be turned around; if starting with a desired BIC, it is possible to design a system that

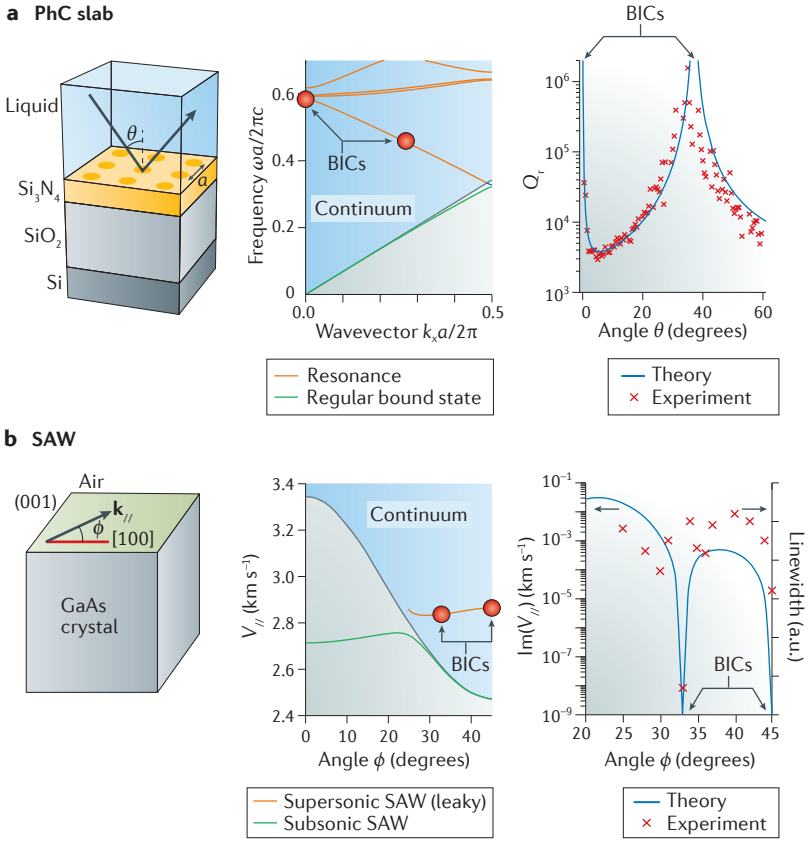

Figure 4 | **Single-resonance parametric BICs. a** | Bound state in the continuum (BIC) from a single resonance in a photonic crystal (PhC) slab. The left panel is a schematic illustration of the system. The middle panel shows the photonic band structure. The leaky resonance turns into two BICs at wavevectors $k_x = 0$ (due to symmetry) and $k_x a/2\pi \approx 0.27$ (through tuning) as marked by red circles. The radiative quality factor, Q_r, diverges to infinity at the two BICs, as shown by the experimental data (red crosses) and theory (blue line) in the right panel. **b** | BIC from the leaky surface acoustic wave (SAW) of GaAs. The left panel is a schematic illustration of the (001) surface of GaAs. The middle panel depicts the acoustic band structure. Radiation of the leaky SAW (orange line) vanishes at $\phi = 45°$ (due to symmetry) and at $\phi \approx 33°$ (through tuning). The right panel shows the theoretical results of attenuation in log scale (blue line) and measured resonance linewidth in linear scale (red crosses). *a*, periodicity; a.u. arbitrary units; *c*, vacuum speed of light; $V_{//}$, phase velocity; $\mathrm{Im}(V_{//})$, imaginary part of the phase velocity. Part **a** is from REF. 132, Nature Publishing Group. Part **b** is adapted with permission from REF. 157, American Institute of Physics, and from REF. 159, Elsevier.

can support this bound state and the continuous spectrum containing it. This inverse construction is achieved by engineering the potential, the hopping rate or the boundary shape of the structure.

Potential engineering. The first proposal of BICs by von Neumann and Wigner was based on potential engineering[3]. For a desired BIC with wave function Ψ and energy $E > 0$, the corresponding potential V can be determined by rewriting the Schrödinger equation (in reduced units):

$$-\frac{1}{2}\nabla^2\Psi + V\Psi = E\Psi \rightarrow V = E + \frac{\nabla^2\Psi}{2\Psi} \qquad (6)$$

Ψ and E must be chosen appropriately so that the resulting V vanishes at infinity (to support the continuum) and is well defined everywhere. There are many possible solutions. The example given by von Neumann and Wigner is $\Psi(\mathbf{r}) = f(r)\sin(kr)/kr$ with $f(r) = [A^2 + (2kr - \sin(2kr))^2]^{-1}$, which has an energy $E = k^2/2$ embedded in the continuum $E \geq 0$. This bound wave function and the corresponding potential $V(\mathbf{r})$ from equation 6 is shown in FIG. 5a for $A = 25$, $k = \sqrt{8}$ and $E = 4$ (note that REF. 3 contains an algebraic mistake[177,178]). More examples can be found in REF. 178, and this procedure has been generalized to non-local potentials[179] and lattice systems[180,181]. From a mathematical point of view, this inverse construction is closely related to the inverse spectral theory of the Schrödinger operator[182] and the Gel'fand–Levitan formalism of the inverse scattering problem, which can also be used to construct potentials supporting a finite[183–186] or even infinite number of BICs[182,187].

A related approach uses the Darboux transformation[188] that is commonly used in supersymmetric (SUSY) quantum mechanics to generate a family of potentials that share the same spectrum. This transformation can be applied to a free-particle extended state to yield a different potential in which the corresponding state keeps its positive energy (remaining in the continuum) but becomes spatially localized[189–191]. In some cases, this SUSY method is equivalent to the von Neumann–Wigner approach and the Gel'fand–Levitan approach[192]. The SUSY method has been applied to generate BICs in point interaction systems[193], periodic Lamé potentials[194] and photonic crystals[195]. The SUSY method has also been extended to non-Hermitian systems with material gain and loss, in which BICs are found below, above and at an exceptional point[196–204].

Potential engineering allows for analytic solutions of BICs. However, the resulting potentials tend to be unrealistic — indeed, none have been realized experimentally so far. In addition, perturbations generally reduce such BICs into ordinary resonances[205,206].

Hopping rate engineering. A more experimentally relevant construction is to engineer the hopping rate between nearest neighbours in a tight-binding lattice model. Such construction can be carried out through the SUSY transformation[199,207] and has been demonstrated in a coupled optical waveguide array, in which the hopping rate is tuned by the distance between neighbouring waveguides[208]. Intuitively, this method can be understood as 'kinetic energy engineering'.

The array of coupled optical waveguides[208] comprises a semi-infinite 1D lattice in which the on-site energy is constant and the hopping rate, κ_n, between sites n and $n+1$ follows (FIG. 5b):

$$\kappa_n = \begin{cases} \kappa & n \neq lN, \\ \left(\dfrac{l+1}{l}\right)^{\beta}\kappa & n = lN,\ (l = 1,2,3,\ldots) \end{cases} \qquad (7)$$

where $N > 1$ is an integer, $\beta > 1/2$ is an arbitrary real number and κ is the reference hopping rate. This system supports $N-1$ BICs localized near the surface ($n = 1$). The particular case of $N = 2$ and $\beta = 1$ was experimentally realized with 40 evanescently coupled optical waveguides[208]. The

Box 2 | **Topological nature of BICs**

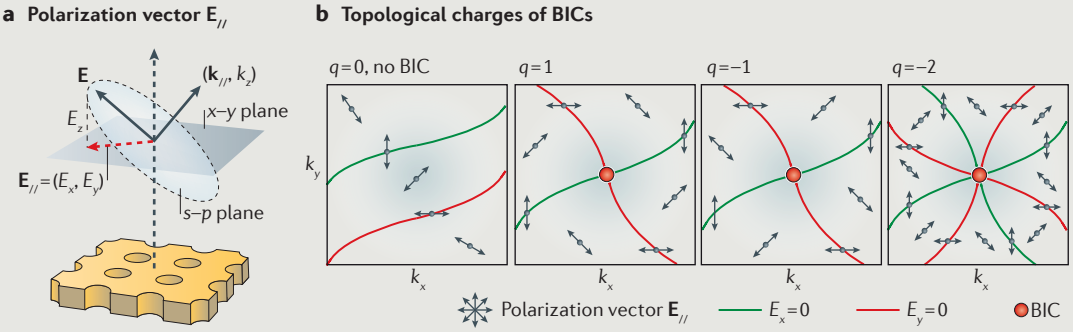

Perturbations typically turn a bound state in the continuum (BIC) into a leaky resonance. However, some BICs are protected topologically and cannot be removed except by large variations in the parameters of the system.

The topological nature of BICs can be understood through the robust BICs in photonic crystal (PhC) slabs, which are fundamentally 2D topological objects[141] — vortices. For a general resonance in a PhC slab, the polarization direction of the far-field radiation is given by a 2D vector, $\mathbf{E}_{//}=(E_x, E_y)$ (part **a**). BICs do not radiate; they exist at the crossing points between the nodal lines of $E_x=0$ and those of $E_y=0$. In the k space, the polarization vector forms a vortex around each BIC with a corresponding 'topological charge', q; a few examples ($q=1$, -1 and -2) are shown in part **b** as well as the case with no BIC ($q=0$). Once any crossing (BIC) occurs, large changes in the system parameters are required to remove it. Topological charges cannot suddenly disappear, because they are conserved and quantized quantities protected by boundary conditions[257]; therefore, a BIC of this type cannot be removed unless it is cancelled out with another BIC carrying the exact opposite topological charge.

The topological properties of BICs were also studied in electron systems with a 2D quantum Hall insulator placed on top of a 3D bulk normal insulator[142]. Under low-energy excitation, pure surface modes in the quantum Hall system were found at isolated k points, embedded in the continuum of the bulk modes of the normal insulator.

Recently, a unified picture of BICs as topological defects has been presented (unpublished observation, H. Zhou). This study shows that the sum of all topological charges carried by the BICs within the Brillouin zone is governed by a different topological invariant of the bands — Chern numbers[258]. The identification and design of BICs in other wave systems, such as polaritons, magnons and anyons, may be possible using this unified theorem.

theoretical hopping rates, the BIC mode intensity, $|c_n|^2$, along with the experimentally measured intensity when light is launched from the first site are shown in FIG. 5b.

Boundary shape engineering. BICs can also arise from engineering the boundary shape of the structure. This method was first proposed in water waves, in a system involving two line sources placed at a certain distance apart on the water surface such that the propagation phase shift is π (REF. 80). Surface-wave radiations from the two sources cancel, resulting in a spatially confined mode profile. Then, the two line sources are replaced with two obstacles whose boundary shapes correspond to streamlines of the mode profile that contain the two sources. In this way, the mode profile in the original driven system is a BIC in the new undriven system with obstacles, because it satisfies the Neumann boundary condition on the obstacle surface, which is a property of the streamlines.

BICs constructed with two line sources or a ring of sources typically lead to the Fabry–Pérot type[80,82,83,111,112] as described earlier. But this procedure can be extended to more complex shapes[209,210] and to free-floating rather than fixed obstacles[211–213].

Applications of BICs and quasi-BICs

Lasing, sensing and filtering. Structures with BICs are natural high-Q resonators, because the Q_r is, in the ideal case, infinity. This makes them useful for many optical and photonic applications. In particular, the macroscopic size (on the centimetre scale or larger) and ease of fabrication make BICs in PhC slabs unique for large-area high-power applications such as lasers[214–219], sensors[220,221] and filters[222].

Many surface-emitting lasers are based on symmetry-protected BICs at the Γ point (FIG. 2c). This effect was first observed by the suppression of radiation into the normal direction in a surface-emitting distributed feedback laser with 1D periodicity[58,59]. This led to PhC surface-emitting lasers (PCSELs) that lase through BICs with 2D periodicity[214,215], followed by the realization of various lasing patterns[216,217], lasing at the blue-violet wavelengths[218] and lasing with organic molecules[221]. The suppressed radiation in the normal direction means that a PCSEL can have a low lasing threshold but also with a limited output power. Therefore, recent designs intentionally break the C_2 symmetry to allow some radiation into the normal direction. For example, the air holes can be intentionally designed as triangular shapes to break the C_2 symmetry (FIG. 6a,b); this led to[219] continuous-wave lasing at room temperature with 1.5 watt output power and high beam quality ($M^2 \leq 1.1$), even though the threshold is still relatively low (FIG. 6c). In addition, PCSELs produce vector beams[223,224] with the order numbers given by the topological charges of the BICs[141] (BOX 2), which may find applications in super-resolution microscopy and in table-top particle accelerators (see REF. 225 for a review on vector beams).

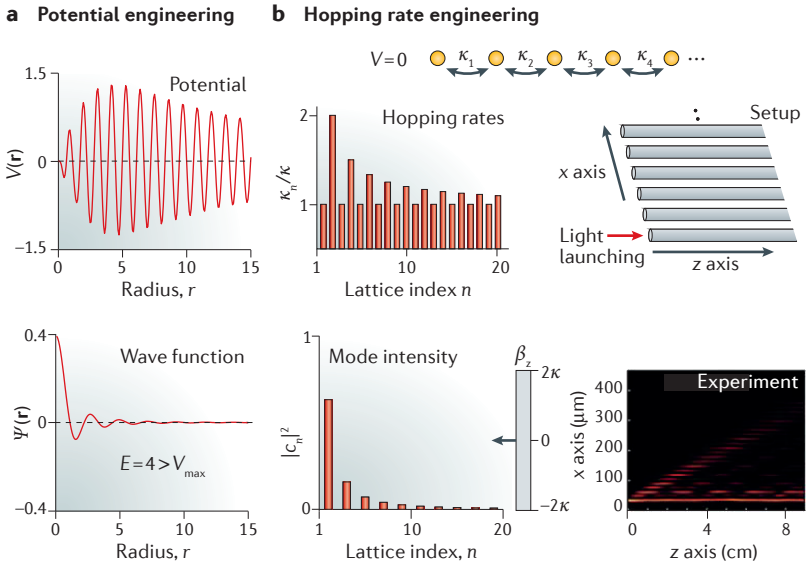

Figure 5 | **A BIC through inverse construction. a** | The bound state in the continuum (BIC) proposed by von Neumann and Wigner[3]. A potential (left panel) is engineered to support a localized electron wave function (right panel) with its energy embedded in the continuous spectrum of extended states. **b** | Construction of a BIC by engineering the hopping rates in a semi-infinite lattice system. The hopping rates κ_n (top left panel) follow equation 7 to support a bound state (bottom left panel) at $\beta_z = 0$, embedded in the continuum of the extended states ($-2\kappa \leq \beta_z \leq 2\kappa$). This BIC is experimentally realized in an array of coupled optical waveguides (top right panel); light launched at one end of the array excites the BIC, which propagates along the waveguides. The corresponding intensity image is shown in the bottom right image. β_z, propagation constant; $|c_n|^2$, BIC mode intensity; E, energy; $\Psi(\mathbf{r})$, wave function; $V(\mathbf{r})$, potential function; V_{max}, maximum potential. Part **b** is adapted with permission from REF. 208, American Physical Society.

Another application lies in chemical and biological sensing, and particularly in optofluidic setups[226]. One sensing mechanism uses the shift of resonance frequency to detect the change of refractive index in the surroundings. Resonators with higher *Q*s enable narrower linewidths and higher sensitivity, and it is possible to directly visualize a single monolayer of proteins with the naked eye using the high-*Q* resonances close to a BIC[220]. Another type of sensing relies on measuring fluorescence signals. More specifically, the spontaneous emission from organic molecules can be strongly enhanced and the angular distribution can be strongly modified near BICs in a PhC slab, leading to a total enhancement of angular fluorescence intensity by 6,300 times[221]. BICs have also permitted large-area narrow-band filters in the infrared regime[222] as a consequence of their high and tunable *Q*s.

Supersonic surface acoustic wave devices. BICs in acoustic wave systems, such as the supersonic SAW on the surface of anisotropic solids (FIG. 4b), have enabled important devices such as supersonic SAW filters. A schematic setup comprising an interdigital transducer placed on a piezoelectric substrate is depicted in FIG. 6d. This device converts the input electric signal into an acoustic wave, which propagates as a SAW to the other side and reverts to an electric signal on the output side. In contrast to a regular subsonic SAW — the speed of which is limited by the speed of the bulk waves — a BIC allows propagation at a much faster supersonic speed (FIG. 6e), and can therefore be used as a supersonic SAW filter. The BIC and supersonic SAW are along a fixed direction ($\phi = 36°$ in FIG. 6f), because other directions are lossy. The spatial periodicity of the interdigital transducer determines $|\mathbf{k}_{//}|$, and the central angular frequency of the SAW filter is given by $\omega = |\mathbf{k}_{//}|V$. A characteristic filtering spectrum[176] using a supersonic SAW filter on Y–X cut $LiTaO_3$ is shown in FIG. 6f. Supersonic SAW filters based on BICs are widely used in mobile phones and cordless phones, Bluetooth devices and delay lines[173–175] because of their low loss, high piezoelectric coupling, reasonable temperature stability, excellent accuracy and repeatability, and compatibility with photolithography[227].

Guiding photons in gapless PhC fibres. PhC fibres can guide light in a low-index material through a photonic bandgap[48], but the bandwidth is limited by the width of the bandgap. A type of hollow-core Kagome-lattice PhC fibre (FIG. 6g) can provide wave guiding inside the continuum without a bandgap[228,229]. Its mechanism — sometimes referred to as inhibited coupling — is a consequence of the dissimilar azimuthal dependence of the core and cladding modes. More specifically, the core mode varies slowly with angle, but the cladding mode is oscillating quickly, as can be seen from the unit-cell mode (FIG. 6h). Although such fibre modes are not true BICs because there can be residual radiation, they enable broadband guidance in air and have found many applications, including multiple-octave frequency comb generations[229] (FIG. 6i), all-fibre gas cells[230,231] and Raman sensing[232]. In addition, by carefully engineering the core shape, the residual radiation of these quasi-BIC modes is reduced significantly to 17 dB km^{-1}, which is comparable to photonic bandgap fibres[233].

Outlook

As a general wave phenomenon, BICs arise through several distinct mechanisms and exist in a wide range of material systems. In this Review, we have described the main mechanisms with examples from atomic and molecular systems, quantum dots, electromagnetic waves, acoustic waves in air, water waves and elastic waves in solids.

We have not covered all possible mechanisms. For example, BICs in systems with chiral symmetry[234] are distinct from the symmetry-protected BICs. In some two-particle Hubbard models, there are bound states that can move into and out of the continuum continuously[235–238]; the confinement requires no parameter tuning and has been credited to integrability[236]. Systems with a perfectly flat band can support localized states[239,240]. Localization can be induced with strong gain and/or loss: for example, in a defect site with high loss[241] and in the bulk[200,202,242,243] or on the surface[244] of parity-time symmetric systems. The latter has been realized in a synthetic photonic lattice[245]. There may also be more constructions not yet discovered.

Even though the very first proposal[3] and many subsequent studies pointed to the existence of BICs in quantum systems, there have not been any conclusive observations of a quantum BIC except for the suppressed linewidth

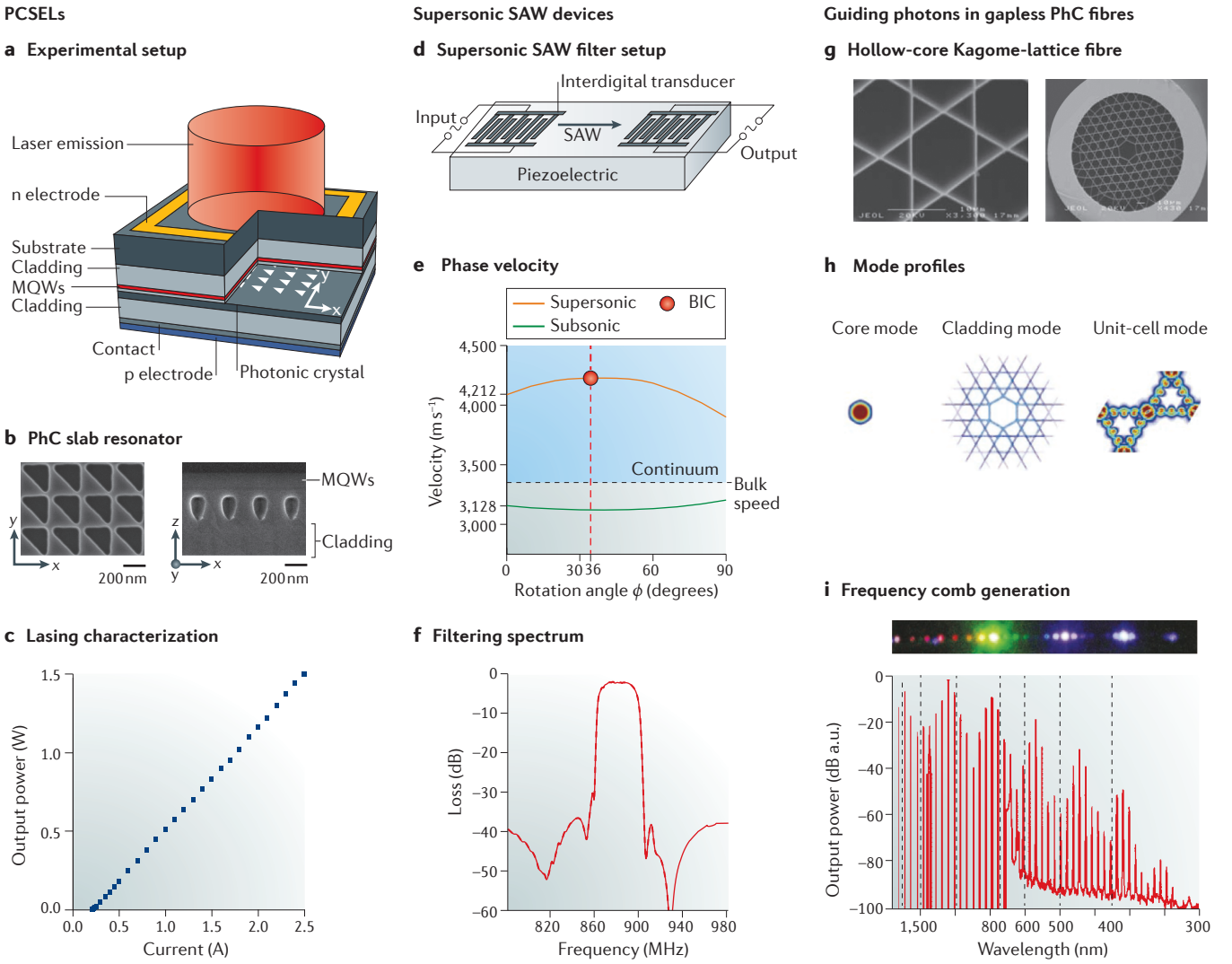

Figure 6 | **Applications of BICs and quasi-BICs. a–c** | Photonic crystal surface-emitting lasers (PCSELs). Schematic representation of the experimental setup (part **a**). The lasing mode is a quasi-bound state in the continuum (BIC) because the 180° rotational symmetry of the photonic crystal (PhC) is broken by the triangular air-hole shapes evident in part **b**. The input–output curve of the PCSEL operating under room-temperature continuous-wave condition demonstrates a low threshold and a high output power (part **c**). **d–f** | Supersonic surface acoustic wave (SAW) filters. Schematic illustration of the setup: two interdigital transducers are placed on a piezoelectric substrate along the direction of the acoustic BIC (part **d**). A comparison between the phase velocities of supersonic and subsonic SAWs on Y–X cut $LiTaO_3$ (part **e**). A BIC appears at $\phi = 36°$, which can be used as a supersonic SAW filter with its characteristic transmission spectrum shown in part **f**. **g–i** | Guiding photons without bandgaps. Scanning electron microscope images of a hollow-core Kagome-lattice PhC fibre are in shown in part **g**. Photonic guiding in such fibres uses quasi-BICs relying on the 'inhibited coupling' between the core and cladding modes, which can be understood from the dissimilar behaviours of the core and unit-cell modes along the azimuthal direction (part **h**). Part **i** is an image and spectrum showing the generation and guidance of a three-octave spectral comb using the quasi-BICs in such fibres. a.u., arbitrary units; MQWs, multiple quantum wells. Parts **a–c** are from REF. 219, Nature Publishing Group. Part **e** is adapted with permission from REF. 227, Academic Press (Elsevier). Part **f** is adapted with permission from REF. 176, © 2002 IEEE. Parts **g–i** are adapted with permission from REF. 229, AAAS.

in Rydberg atoms[120]. Many researchers mistakenly cite REF. 246 as an experimental realization of a quantum BIC, but this study concerns a positive-energy defect state with energy in the bandgap created by a superlattice, not a BIC. A quantum BIC has been claimed in a study on multiple quantum wells[247]; however, data indicate a finite leakage rate and no evidence for localization. The difficulty arises from the relatively few control parameters and the large number of decay pathways in quantum systems. Therefore, the realization of a quantum BIC remains a challenge.

Optical systems provide a clean and versatile platform for realizing different types of BICs[27,28,49,57,110,132,208,245], because of nanofabrication technologies that enable the creation of customized photonic structures. An optical BIC exhibits an ultrahigh Q — its Q_r is technically

infinity — which can increase the interaction time between light and matter by orders of magnitude. In addition to the high-*Q* applications described above, there are many more opportunities in, for example, nonlinearity enhancement and quantum optical applications that have not been explored. The long-range interactions in Fabry–Pérot BICs may be useful for nanophotonic circuits[104] and for quantum information processing[105,106]. It has also been proposed that the light intensity may act as a tuning parameter in nonlinear materials, which may enable robust BICs[248], tunable channel dropping[249], light storage and release[250,251], and frequency comb generation[252]. Finally, it was shown that particle statistics can be used to modify properties of BICs[253].

Considering the many types of BICs, a natural question is whether a common concept underlies them all other than the vanishing of coupling to radiation through interference. To this end, the topological interpretation of BICs (see BOX 2 and REFS 141,142) seems promising. The topological arguments may guide the discovery of BICs and new ways to trap waves, which may also exist in quasi-particle systems such as magnons, polaritons, polarons and anyons. Because BICs defy conventional wisdom and provide new ways to confine waves, their realization in different material systems are certain to provide even more surprises and advances in both fundamental physics and technological applications.

1. Moiseyev, N. *Non-Hermitian Quantum Mechanics* Ch. 4 (Cambridge Univ. Press, 2011).
2. Kukulin, V. I., Krasnopol'sky, V. M. & Horáček, J. *Theory of Resonances: Principles and Applications* Ch. 2 (Springer, 1989).
3. von Neumann, J. & Wigner, E. Über merkwürdige diskrete Eigenwerte. *Phys. Z.* **30**, 465–467 (in German) (1929).
This paper proposes the possibility of BICs using an engineered quantum potential as an example.
4. Parker, R. Resonance effects in wake shedding from parallel plates: some experimental observations. *J. Sound Vib.* **4**, 62–72 (1966).
This paper reports the observation of symmetry-protected BICs in acoustic waveguides.
5. Parker, R. Resonance effects in wake shedding from parallel plates: calculation of resonant frequencies. *J. Sound Vib.* **5**, 330–343 (1967).
6. Cumpsty, N. A. & Whitehead, D. S. The excitation of acoustic resonances by vortex shedding. *J. Sound Vib.* **18**, 353–369 (1971).
7. Koch, W. Resonant acoustic frequencies of flat plate cascades. *J. Sound Vib.* **88**, 233–242 (1983).
8. Parker, R. & Stoneman, S. A. T. The excitation and consequences of acoustic resonances in enclosed fluid flow around solid bodies. *Proc. Inst. Mech. Eng. C* **203**, 9–19 (1989).
9. Evans, D. V., Levitin, M. & Vassiliev, D. Existence theorems for trapped modes. *J. Fluid Mech.* **261**, 21–31 (1994).
10. Evans, D. V., Linton, C. M. & Ursell, F. Trapped mode frequencies embedded in the continuous spectrum. *Q. J. Mech. Appl. Math.* **46**, 253–274 (1993).
11. Groves, M. D. Examples of embedded eigenvalues for problems in acoustic waveguides. *Math. Meth. Appl. Sci.* **21**, 479–488 (1998).
12. Linton, C. & McIver, M. Trapped modes in cylindrical waveguides. *Q. J. Mech. Appl. Math.* **51**, 389–412 (1998).
13. Davies, E. & Parnovski, L. Trapped modes in acoustic waveguides. *Q. J. Mech. Appl. Math.* **51**, 477–492 (1998).
14. Ursell, F. Trapping modes in the theory of surface waves. *Math. Proc. Cambridge Philos. Soc.* **47**, 347–358 (1951).
15. Jones, D. S. The eigenvalues of $\nabla^2 u + \lambda u = 0$ when the boundary conditions are given on semi-infinite domains. *Math. Proc. Cambridge Philos. Soc.* **49**, 668–684 (1953).
16. Callan, M., Linton, C. M. & Evans, D. V. Trapped modes in two-dimensional waveguides. *J. Fluid Mech.* **229**, 51–64 (1991).
17. Retzler, C. H. Trapped modes: an experimental investigation. *Appl. Ocean Res.* **23**, 249–250 (2001).
18. Cobelli, P. J., Pagneux, V., Maurel, A. & Petitjeans, P. Experimental observation of trapped modes in a water wave channel. *Euro. Phys. Lett.* **88**, 20006 (2009).
19. Cobelli, P. J., Pagneux, V., Maurel, A. & Petitjeans, P. Experimental study on water-wave trapped modes. *J. Fluid Mech.* **666**, 445–476 (2011).
20. Pagneux, V. in *Dynamic Localization Phenomena in Elasticity, Acoustics and Electromagnetism* (eds Craster, R. & Kaplunov, J.) 181–223 (Springer, 2013).
21. Schult, R. L., Ravenhall, D. G. & Wyld, H. W. Quantum bound states in a classically unbound system of crossed wires. *Phys. Rev. B* **39**, 5476–5479 (1989).
22. Exner, P., Šeba, P., Tater, M. & Vaněk, D. Bound states and scattering in quantum waveguides coupled laterally through a boundary window. *J. Math. Phys.* **37**, 4867–4887 (1996).
23. Moiseyev, N. Suppression of Feshbach resonance widths in two-dimensional waveguides and quantum dots: a lower bound for the number of bound states in the continuum. *Phys. Rev. Lett.* **102**, 167404 (2009).
24. Cederbaum, L. S., Friedman, R. S., Ryaboy, V. M. & Moiseyev, N. Conical intersections and bound molecular states embedded in the continuum. *Phys. Rev. Lett.* **90**, 013001 (2003).
25. Longhi, S. Transfer of light waves in optical waveguides via a continuum. *Phys. Rev. A* **78**, 013815 (2008).
26. Longhi, S. Optical analog of population trapping in the continuum: classical and quantum interference effects. *Phys. Rev. A* **79**, 023811 (2009).
27. Dreisow, F. *et al.* Adiabatic transfer of light via a continuum in optical waveguides. *Opt. Lett.* **34**, 2405–2407 (2009).
This paper realizes light transfer based on symmetry-protected and Fabry–Pérot BICs in a coupled-waveguide array.
28. Plotnik, Y. *et al.* Experimental observation of optical bound states in the continuum. *Phys. Rev. Lett.* **107**, 183901 (2011).
This paper realizes an optical symmetry-protected BIC in a coupled-waveguide array.
29. Shipman, S. P., Ribbeck, J., Smith, K. H. & Weeks, C. A. Discrete model for resonance near embedded bound states. *IEEE Photonics J.* **2**, 911–923 (2010).
30. Ptitsyna, N. & Shipman, S. P. A lattice model for resonance in open periodic waveguides. *Discrete Contin. Dyn. Syst. S* **5**, 989–1020 (2012).
31. Ladrón de Guevara, M. L., Claro, F. & Orellana, P. A. Ghost Fano resonance in a double quantum dot molecule attached to leads. *Phys. Rev. B* **67**, 195335 (2003).
32. Orellana, P. A., Ladrón de Guevara, M. L. & Claro, F. Controlling Fano and Dicke effects via a magnetic flux in a two-site Anderson model. *Phys. Rev. B* **70**, 233315 (2004).
33. Ladrón de Guevara, M. L. & Orellana, P. A. Electronic transport through a parallel-coupled triple quantum dot molecule: Fano resonances and bound states in the continuum. *Phys. Rev. B* **73**, 205303 (2006).
34. Voo, K.-K. & Chu, C. S. Localized states in continuum in low-dimensional systems. *Phys. Rev. B* **74**, 155306 (2006).
35. Solís, B., Ladrón de Guevara, M. L. & Orellan, P. A. Friedel phase discontinuity and bound states in the continuum in quantum dot systems. *Phys. Lett. A* **372**, 4736–4739 (2008).
36. Gong, W., Han, Y. & Wei, G. Antiresonance and bound states in the continuum in electron transport through parallel-coupled quantum-dot structures. *J. Phys. Condens. Matter* **21**, 175801 (2009).
37. Han, Y., Gong, W. & Wei, G. Bound states in the continuum in electronic transport through parallel-coupled quantum-dot structures. *Phys. Status Solidi B* **246**, 1634–1641 (2009).
38. Vallejo, M. L., Ladrón de Guevara, M. L. & Orellana, P. A. Triple Rashba dots as a spin filter: bound states in the continuum and Fano effect. *Phys. Lett. A* **374**, 4928–4932 (2010).
39. Yan, J.-X. & Fu, H.-H. Bound states in the continuum and Fano antiresonance in electronic transport through a four-quantum-dot system. *Phys. B* **410**, 197–200 (2013).
40. Ramos, J. P. & Orellana, P. A. Bound states in the continuum and spin filter in quantum-dot molecules. *Phys. B* **455**, 66–70 (2014).
41. Álvarez, C., Domínguez-Adame, F., Orellana, P. A. & Díaz, E. Impact of electron–vibron interaction on the bound states in the continuum. *Phys. Lett. A* **379**, 1062–1066 (2015).
42. González, J. W., Pacheco, M., Rosales, L. & Orellana, P. A. Bound states in the continuum in graphene quantum dot structures. *Euro. Phys. Lett.* **91**, 66001 (2010).
43. Cortés, N., Chico, L., Pacheco, M., Rosales, L. & Orellana, P. A. Bound states in the continuum: localization of Dirac-like fermions. *Euro. Phys. Lett.* **108**, 46008 (2014).
44. Bulgakov, E. N., Pichugin, K. N., Sadreev, A. F. & Rotter, I. Bound states in the continuum in open Aharonov–Bohm rings. *JETP Lett.* **84**, 430–435 (2006).
45. Voo, K.-K. Trapped electromagnetic modes in forked transmission lines. *Wave Motion* **45**, 795–803 (2008).
46. Guessi, L. H. *et al.* Catching the bound states in the continuum of a phantom atom in graphene. *Phys. Rev. B* **92**, 045409 (2015).
47. Guessi, L. H. *et al.* Quantum phase transition triggering magnetic bound states in the continuum in graphene. *Phys. Rev. B* **92**, 245107 (2015).
48. Joannopoulos, J. D., Johnson, S. G., Winn, J. N. & Meade, R. D. *Photonic Crystals: Molding the Flow of Light* Ch. 8,9 (Princeton Univ. Press, 2008).
49. Ulrich, R. in *Symposium on optical and acoustical micro-electronics* (ed. Fox, J.) 359–376 (New York,1975).
This work observes a symmetry-protected BIC in a periodic metal grid.
50. Bonnet-Bendhia, A.-S. & Starling, F. Guided waves by electromagnetic gratings and non-uniqueness examples for the diffraction problem. *Math. Meth. Appl. Sci.* **17**, 305–338 (1994).
51. Paddon, P. & Young, J. F. Two-dimensional vector-coupled-mode theory for textured planar waveguides. *Phys. Rev. B* **61**, 2090–2101 (2000).
52. Pacradouni, V. *et al.* Photonic band structure of dielectric membranes periodically textured in two dimensions. *Phys. Rev. B* **62**, 4204–4207 (2000).
53. Ochiai, T. & Sakoda, K. Dispersion relation and optical transmittance of a hexagonal photonic crystal slab. *Phys. Rev. B* **63**, 125107 (2001).
54. Fan, S. & Joannopoulos, J. D. Analysis of guided resonances in photonic crystal slabs. *Phys. Rev. B* **65**, 235112 (2002).
55. Tikhodeev, S. G., Yablonskii, A. L., Muljarov, E. A., Gippius, N. A. & Ishihara, T. Quasiguided modes and optical properties of photonic crystal slabs. *Phys. Rev. B* **66**, 045102 (2002).
56. Shipman, S. P. & Venakides, S. Resonant transmission near nonrobust periodic slab modes. *Phys. Rev. E* **71**, 026611 (2005).
57. Lee, J. *et al.* Observation and differentiation of unique high-*Q* optical resonances near zero wave vector in macroscopic photonic crystal slabs. *Phys. Rev. Lett.* **109**, 067401 (2012).

58. Henry, C. H., Kazarinov, R. F., Logan, R. A. & Yen, R. Observation of destructive interference in the radiation loss of second-order distributed feedback lasers. *IEEE J. Quantum Electron.* **21**, 151–154 (1985).
This paper demonstrates lasing through a symmetry-protected BIC in a distributed feedback laser with 1D periodicity.
59. Kazarinov, R. F. & Henry, C. H. Second-order distributed feedback lasers with mode selection provided by first-order radiation losses. *IEEE J. Quantum Electron.* **21**, 144–150 (1985).
60. Lim, T. C. & Farnell, G. W. Character of pseudo surface waves on anisotropic crystals. *J. Acoust. Soc. Am.* **45**, 845–851 (1969).
61. Farnell, G. W. in *Physical Acoustics* Vol. 6 (eds Mason, W. P. & Thurston, R. N.) 109–166 (Academic Press, 1970).
62. Alshits, V. I. & Lothe, J. Comments on the relation between surface wave theory and the theory of reflection. *Wave Motion* **3**, 297–310 (1981).
63. Chadwick, P. The behaviour of elastic surface waves polarized in a plane of material symmetry I. General analysis. *Proc. R. Soc. A* **430**, 213–240 (1990).
64. Alshits, V. I., Darinskii, A. N. & Shuvalov, A. L. Elastic waves in infinite and semi-infinite anisotropic media. *Phys. Scr.* **1992**, 85 (1992).
65. Shipman, S. P. & Welters, A. in *Proceedings of the 2012 international conference on mathematical methods in electromagnetic theory (MMET)* 227–232 (Kharkiv, 2012).
66. Robnik, M. A simple separable Hamiltonian having bound states in the continuum. *J. Phys. A* **19**, 3845 (1986).
This paper proposes BICs in a quantum well based on separability.
67. Nockel, J. U. Resonances in quantum-dot transport. *Phys. Rev. B* **46**, 15348 (1992).
68. Duclos, P., Exner, P. & Meller, B. Open quantum dots: resonances from perturbed symmetry and bound states in strong magnetic fields. *Rep. Math. Phys.* **47**, 253–267 (2001).
69. Prodanovič, N., Milanovič, V., Ikonič, Z., Indjin, D. & Harrison, P. Bound states in continuum: quantum dots in a quantum well. *Phys. Lett. A* **377**, 2177–2181 (2013).
70. Čtyroký, J. Photonic bandgap structures in planar waveguides. *J. Opt. Soc. Am. A* **18**, 435–441 (2001).
71. Kawakami, S. Analytically solvable model of photonic crystal structures and novel phenomena. *J. Lightwave Technol.* **20**, 1644–1650 (2002).
72. Watts, M. R., Johnson, S. G., Haus, H. A. & Joannopoulos, J. D. Electromagnetic cavity with arbitrary *Q* and small modal volume without a complete photonic bandgap. *Opt. Lett.* **27**, 1785–1787 (2002).
73. Apalkov, V. M. & Raikh, M. E. Strongly localized mode at the intersection of the phase slips in a photonic crystal without band gap. *Phys. Rev. Lett.* **90**, 253901 (2003).
74. Rivera, N. *et al.* Controlling directionality and dimensionality of radiation by perturbing separable bound states in the continuum. Preprint at http://arxiv.org/abs/1507.00923 (2016).
75. Fan, S., Suh, W. & Joannopoulos, J. D. Temporal coupled-mode theory for the Fano resonance in optical resonators. *J. Opt. Soc. Am. A* **20**, 569–572 (2003).
76. Haus, H. A. *Waves and Fields in Optoelectronics* Ch. 7 (Prentice-Hall, 1984).
77. Fan, S. *et al.* Theoretical analysis of channel drop tunneling processes. *Phys. Rev. B* **59**, 15882–15892 (1999).
78. Manolatou, C. *et al.* Coupling of modes analysis of resonant channel add-drop filters. *IEEE J. Quantum Electron.* **35**, 1322–1331 (1999).
79. Wang, Z. & Fan, S. Compact all-pass filters in photonic crystals as the building block for high-capacity optical delay lines. *Phys. Rev. E* **68**, 066616 (2003).
80. McIver, M. An example of non-uniqueness in the two-dimensional linear water wave problem. *J. Fluid Mech.* **315**, 257–266 (1996).
This paper proposes a Fabry–Pérot BIC for water waves by engineering the shapes of two obstacles.
81. Linton, C. M. & Kuznetsov, N. G. Non-uniqueness in two-dimensional water wave problems: numerical evidence and geometrical restrictions. *Proc. R. Soc. A* **453**, 2437–2460 (1997).
82. Evans, D. V. & Porter, R. An example of non-uniqueness in the two-dimensional linear water-wave problem involving a submerged body. *Proc. R. Soc. A* **454**, 3145–3165 (1998).
83. McIver, M. Trapped modes supported by submerged obstacles. *Proc. R. Soc. A* **456**, 1851–1860 (2000).
84. Kuznetsov, N., McIver, P. & Linton, C. M. On uniqueness and trapped modes in the water-wave problem for vertical barriers. *Wave Motion* **33**, 283–307 (2001).
85. Porter, R. Trapping of water waves by pairs of submerged cylinders. *Proc. R. Soc. A* **458**, 607–624 (2002).
86. Linton, C. M. & McIver, P. Embedded trapped modes in water waves and acoustics. *Wave Motion* **45**, 16–29 (2007).
This paper reviews theoretical studies of BICs in acoustic and water waves.
87. Shahbazyan, T. V. & Raikh, M. E. Two-channel resonant tunneling. *Phys. Rev. B* **49**, 17123–17129 (1994).
88. Kim, C. S. & Satanin, A. M. Dynamic confinement of electrons in time-dependent quantum structures. *Phys. Rev. B* **58**, 15389–15392 (1998).
89. Rotter, I. & Sadreev, A. F. Zeros in single-channel transmission through double quantum dots. *Phys. Rev. E* **71**, 046204 (2005).
90. Sadreev, A. F., Bulgakov, E. N. & Rotter, I. Trapping of an electron in the transmission through two quantum dots coupled by a wire. *JETP Lett.* **82**, 498–503 (2005).
91. Ordonez, G., Na, K. & Kim, S. Bound states in the continuum in quantum-dot pairs. *Phys. Rev. A* **73**, 022113 (2006).
92. Tanaka, S., Garmon, S., Ordonez, G. & Petrosky, T. Electron trapping in a one-dimensional semiconductor quantum wire with multiple impurities. *Phys. Rev. B* **76**, 153308 (2007).
93. Cattapan, G. & Lotti, P. Bound states in the continuum in two-dimensional serial structures. *Eur. Phys. J. B* **66**, 517–523 (2008).
94. Díaz-Tendero, S., Borisov, A. G. & Gauyacq, J.-P. Extraordinary electron propagation length in a metallic double chain supported on a metal surface. *Phys. Rev. Lett.* **102**, 166807 (2009).
95. Sadreev, A. F., Maksimov, D. N. & Pilipchuk, A. S. Gate controlled resonant widths in double-bend waveguides: bound states in the continuum. *J. Phys. Condens. Matter* **27**, 295303 (2015).
96. Suh, W., Yanik, M. F., Solgaard, O. & Fan, S. Displacement-sensitive photonic crystal structures based on guided resonance in photonic crystal slabs. *Appl. Phys. Lett.* **82**, 1999–2001 (2003).
97. Suh, W., Solgaard, O. & Fan, S. Displacement sensing using evanescent tunneling between guided resonances in photonic crystal slabs. *J. Appl. Phys.* **98**, 033102 (2005).
98. Liu, V., Povinelli, M. & Fan, S. Resonance-enhanced optical forces between coupled photonic crystal slabs. *Opt. Express* **17**, 21897–21909 (2009).
99. Marinica, D. C., Borisov, A. G. & Shabanov, S. V. Bound states in the continuum in photonics. *Phys. Rev. Lett.* **100**, 183902 (2008).
100. Ndangali, R. F. & Shabanov, S. V. Electromagnetic bound states in the radiation continuum for periodic double arrays of subwavelength dielectric cylinders. *J. Math. Phys.* **51**, 102901 (2010).
101. Bulgakov, E. N. & Sadreev, A. F. Bound states in the continuum in photonic waveguides inspired by defects. *Phys. Rev. B* **78**, 075105 (2008).
102. Longhi, S. Optical analogue of coherent population trapping via a continuum in optical waveguide arrays. *J. Mod. Opt.* **56**, 729–737 (2009).
103. Hein, S., Koch, W. & Nannen, L. Trapped modes and Fano resonances in two-dimensional acoustical duct-cavity systems. *J. Fluid Mech.* **692**, 257–287 (2012).
104. Sato, Y. *et al.* Strong coupling between distant photonic nanocavities and its dynamic control. *Nat. Photonics* **6**, 56–61 (2012).
105. Zheng, H. & Baranger, H. U. Persistent quantum beats and long-distance entanglement from waveguide-mediated interactions. *Phys. Rev. Lett.* **110**, 113601 (2013).
106. van Loo, A. F. *et al.* Photon-mediated interactions between distant artificial atoms. *Science* **342**, 1494–1496 (2013).
107. Peleg, O., Plotnik, Y., Moiseyev, N., Cohen, O. & Segev, M. Self-trapped leaky waves and their interactions. *Phys. Rev. A* **80**, 041801 (2009).
108. Hsu, C. W. *et al.* Bloch surface eigenstates within the radiation continuum. *Light Sci. Appl.* **2**, e84 (2013).
109. Longhi, S. Bound states in the continuum in a single-level Fano–Anderson model. *Eur. Phys. J. B* **57**, 45–51 (2007).
110. Weimann, S. *et al.* Compact surface Fano states embedded in the continuum of waveguide arrays. *Phys. Rev. Lett.* **111**, 240403 (2013).
This work realizes a Fabry–Pérot BIC in a coupled-waveguide array.
111. McIver, P. & McIver, M. Trapped modes in an axisymmetric water-wave problem. *Q. J. Mech. Appl. Math.* **50**, 165–178 (1997).
112. Kuznetsov, N. & McIver, P. On uniqueness and trapped modes in the water-wave problem for a surface-piercing axisymmetric body. *Q. J. Mech. Appl. Math.* **50**, 565–580 (1997).
113. Suh, W., Wang, Z. & Fan, S. Temporal coupled-mode theory and the presence of non-orthogonal modes in lossless multimode cavities. *IEEE J. Quantum Electron.* **40**, 1511–1518 (2004).
114. Devdariani, A. Z., Ostrovskii, V. N. & Sebyakin, Y. N. Crossing of quasistationary levels. *Sov. Phys. JETP* **44**, 477 (1976).
115. Friedrich, H. & Wintgen, D. Interfering resonances and bound states in the continuum. *Phys. Rev. A* **32**, 3231–3242 (1985).
This paper proposes that a BIC can arise from two interfering resonances.
116. Remacle, F., Munster, M., Pavlov-Verevkin, V. B. & Desouter-Lecomte, M. Trapping in competitive decay of degenerate states. *Phys. Lett. A* **145**, 265–268 (1990).
117. Berkovits, R., von Oppen, F. & Kantelhardt, J. W. Discrete charging of a quantum dot strongly coupled to external leads. *Euro. Phys. Lett.* **68**, 699 (2004).
118. Fonda, L. & Newton, R. G. Theory of resonance reactions. *Ann. Phys.* **10**, 490–515 (1960).
119. Friedrich, H. & Wintgen, D. Physical realization of bound states in the continuum. *Phys. Rev. A* **31**, 3964–3966 (1985).
120. Neukammer, J. *et al.* Autoionization inhibited by internal interferences. *Phys. Rev. Lett.* **55**, 1979–1982 (1985).
121. Volya, A. & Zelevinsky, V. Non-Hermitian effective Hamiltonian and continuum shell model. *Phys. Rev. C* **67**, 054322 (2003).
122. Deb, B. & Agarwal, G. S. Creation and manipulation of bound states in the continuum with lasers: applications to cold atoms and molecules. *Phys. Rev. A* **90**, 063417 (2014).
123. Sablikov, V. A. & Sukhanov, A. A. Helical bound states in the continuum of the edge states in two dimensional topological insulators. *Phys. Lett. A* **379**, 1775–1779 (2015).
124. Texier, C. Scattering theory on graphs: II. The Friedel sum rule. *J. Phys. A* **35**, 3389 (2002).
125. Sadreev, A. F., Bulgakov, E. N. & Rotter, I. Bound states in the continuum in open quantum billiards with a variable shape. *Phys. Rev. B* **73**, 235342 (2006).
126. Sadreev, A. F. & Babushkina, T. V. Two-electron bound states in a continuum in quantum dots. *JETP Lett.* **88**, 312–317 (2008).
127. Boretz, Y., Ordonez, G., Tanaka, S. & Petrosky, T. Optically tunable bound states in the continuum. *Phys. Rev. A* **90**, 023853 (2014).
128. Lyapina, A. A., Maksimov, D. N., Pilipchuk, A. S. & Sadreev, A. F. Bound states in the continuum in open acoustic resonators. *J. Fluid Mech.* **780**, 370–387 (2015).
129. Lepetit, T., Akmansoy, E., Ganne, J.-P. & Lourtioz, J.-M. Resonance continuum coupling in high-permittivity dielectric metamaterials. *Phys. Rev. B* **82**, 195307 (2010).
130. Lepetit, T. & Kanté, B. Controlling multipolar radiation with symmetries for electromagnetic bound states in the continuum. *Phys. Rev. B* **90**, 241103 (2014).
131. Gentry, C. M. & Popović, M. A. Dark state lasers. *Opt. Lett.* **39**, 4136–4139 (2014).
132. Hsu, C. W. *et al.* Observation of trapped light within the radiation continuum. *Nature* **499**, 188–191 (2013).
This work realizes a single-resonance parametric BIC in a PhC slab.
133. Gansch, R. *et al.* Measurement of bound states in the continuum by a detector embedded in a photonic crystal. *Light Sci. Appl.* http://dx.doi.org/10.1038/lsa.2016.147 (2016).
134. Evans, D. V. & Porter, R. On the existence of embedded surface waves along arrays of parallel plates. *Q. J. Mech. Appl. Math.* **55**, 481–494 (2002).
135. Porter, R. & Evans, D. V. Embedded Rayleigh–Bloch surface waves along periodic rectangular arrays. *Wave Motion* **43**, 29–50 (2005).
136. Bulgakov, E. N. & Sadreev, A. F. Bloch bound states in the radiation continuum in a periodic array of dielectric rods. *Phys. Rev. A* **90**, 053801 (2014).
137. Bulgakov, E. N. & Sadreev, A. F. Light trapping above the light cone in a one-dimensional array of dielectric spheres. *Phys. Rev. A* **92**, 023816 (2015).

138. Longhi, S. & Della Valle, G. Floquet bound states in the continuum. *Sci. Rep.* **3**, 2219 (2013).
139. Yang, Y., Peng, C., Liang, Y., Li, Z. & Noda, S. Analytical perspective for bound states in the continuum in photonic crystal slabs. *Phys. Rev. Lett.* **113**, 037401 (2014).
140. Gao, X. *et al.* Formation mechanism of guided resonances and bound states in the continuum in photonic crystal slabs. Preprint at http://arxiv.org/abs/1603.02815 (2016).
141. Zhen, B., Hsu, C. W., Lu, L., Stone, A. D. & Soljac˘ic´, M. Topological nature of optical bound states in the continuum. *Phys. Rev. Lett.* **113**, 257401 (2014).
This paper explains the topological nature of BICs in PhC slabs.
142. Yang, B.-J., Bahramy, M. S. & Nagaosa, N. Topological protection of bound states against the hybridization. *Nat. Commun.* **4**, 1524 (2013).
143. Linton, C. M., McIver, M., McIver, P., Ratcliffe, K. & Zhang, J. Trapped modes for off-centre structures in guides. *Wave Motion* **36**, 67–85 (2002).
144. Evans, D. & Porter, R. Trapped modes embedded in the continuous spectrum. *Q. J. Mech. Appl. Math.* **51**, 263–274 (1998).
145. McIver, M., Linton, C. M., McIver, P., Zhang, J. & Porter, R. Embedded trapped modes for obstacles in two-dimensional waveguides. *Q. J. Mech. Appl. Math.* **54**, 273–293 (2001).
146. McIver, M., Linton, C. M. & Zhang, J. The branch structure of embedded trapped modes in two-dimensional waveguides. *Q. J. Mech. Appl. Math.* **55**, 313–326 (2002).
147. Koch, W. Acoustic resonances in rectangular open cavities. *AIAA J.* **43**, 2342–2349 (2005).
148. Duan, Y., Koch, W., Linton, C. M. & McIver, M. Complex resonances and trapped modes in ducted domains. *J. Fluid Mech.* **571**, 119–147 (2007).
149. Kim, C. S., Satanin, A. M., Joe, Y. S. & Cosby, R. M. Resonant tunneling in a quantum waveguide: effect of a finite-size attractive impurity. *Phys. Rev. B* **60**, 10962–10970 (1999).
150. Linton, C. M. & Ratcliffe, K. Bound states in coupled guides. I. Two dimensions. *J. Math. Phys.* **45**, 1359–1379 (2004).
151. Cattapan, G. & Lotti, P. Fano resonances in stubbed quantum waveguides with impurities. *Eur. Phys. J. B* **60**, 51–60 (2007).
152. Olendski, O. & Mikhailovska, L. Bound-state evolution in curved waveguides and quantum wires. *Phys. Rev. B* **66**, 035331 (2002).
153. Olendski, O. & Mikhailovska, L. Fano resonances of a curved waveguide with an embedded quantum dot. *Phys. Rev. B* **67**, 035310 (2003).
154. Chen, Y. *et al.* Mechanical bound state in the continuum for optomechanical microresonators. *New J. Phys.* **18**, 063031 (2016).
155. Zou, C.-L. *et al.* Guiding light through optical bound states in the continuum for ultrahigh-*Q* microresonators. *Laser Photon. Rev.* **9**, 114–119 (2015).
156. Penunuri, D. & Lakin, K. M. in *1975 IEEE Ultrason. Symp.* 478–483 (IEEE, Los Angeles, 1975).
157. Stegeman, G. I. Normal-mode surface waves in the pseudobranch on the (001) plane of gallium arsenide. *J. Appl. Phys.* **47**, 1712–1713 (1976).
158. Aleksandrov, V. V. *et al.* New data concerning surface Mandelstamm–Brillouin light scattering from the basal plane of germanium crystal. *Phys. Lett. A* **162**, 418–422 (1992).
159. Aleksandrov, V. V., Velichkina, T. S., Potapova, J. B. & Yakovlev, I. A. Mandelstamm–Brillouin studies of peculiarities of the phonon frequency distribution at cubic crystal (001) surfaces. *Phys. Lett. A* **171**, 103–106 (1992).
160. Taylor, D. B. Surface waves in anisotropic media: the secular equation and its numerical solution. *Proc. R. Soc. A* **376**, 265–300 (1981).
161. Gundersen, S. A., Wang, L. & Lothe, J. Secluded supersonic elastic surface waves. *Wave Motion* **14**, 129–143 (1991).
162. Barnett, D. M., Chadwick, P. & Lothe, J. The behaviour of elastic surface waves polarized in a plane of material symmetry. I. Addendum. *Proc. R. Soc. A* **433**, 699–710 (1991).
163. Maznev, A. A. & Every, A. G. Secluded supersonic surface waves in germanium. *Phys. Lett. A* **197**, 423–427 (1995).
164. Darinskii, A. N., Alshits, V. I., Lothe, J., Lyubimov, V. N. & Shuvalov, A. L. An existence criterion for the branch of two-component surface waves in anisotropic elastic media. *Wave Motion* **28**, 241–257 (1998).
165. Xu, Y. & Aizawa, T. Pseudo surface wave on the (1012) plane of sapphire. *J. Appl. Phys.* **86**, 6507–6511 (1999).
166. Maznev, A. A., Lomonosov, A. M., Hess, P. & Kolomenskii, A. Anisotropic effects in surface acoustic wave propagation from a point source in a crystal. *Eur. Phys. J. B* **35**, 429–439 (2003).
167. Trzupek, D. & Zieliński, P. Isolated true surface wave in a radiative band on a surface of a stressed auxetic. *Phys. Rev. Lett.* **103**, 075504 (2009).
168. Every, A. G. Supersonic surface acoustic waves on the 001 and 110 surfaces of cubic crystals. *J. Acoust. Soc. Am.* **138**, 2937–2944 (2015).
169. Every, A. G. Guided elastic waves at a periodic array of thin coplanar cavities in a solid. *Phys. Rev. B* **78**, 174104 (2008).
170. Maznev, A. A. & Every, A. G. Surface acoustic waves in a periodically patterned layered structure. *J. Appl. Phys.* **106**, 113531 (2009).
171. Every, A. G. & Maznev, A. A. Elastic waves at periodically-structured surfaces and interfaces of solids. *AIP Adv.* **4**, 124401 (2014).
172. Yamanouchi, K. & Shibayama, K. Propagation and amplification of rayleigh waves and piezoelectric leaky surface waves in $LiNbO_3$. *J. Appl. Phys.* **43**, 856–862 (1972).
This work predicts and measures an acoustic single-resonance parametric BIC on the surface of a piezoelectric solid.
173. Lewis, M. F. Acoustic wave devices employing surface skimming bulk waves. US Patent 4159435 (1979).
174. Ueda, M. *et al.* Surface acoustic wave device using a leaky surface acoustic wave with an optimized cut angle of a piezoelectric substrate. US Patent 6037847 (2000).
175. Kawachi, O. *et al.* Optimal cut for leaky SAW on $LiTaO_3$ for high performance resonators and filters. *IEEE Trans. Ultrason. Ferroelectr. Freq. Control* **48**, 1442–1448 (2001).
176. Naumenko, N. & Abbot, B. in *Proc. 2002 IEEE Ultrason. Symp.* **1**, 385–390 (IEEE, 2002).
177. Simon, B. On positive eigenvalues of one-body Schrödinger operators. *Commun. Pure Appl. Math.* **22**, 531–538 (1969).
178. Stillinger, F. H. & Herrick, D. R. Bound states in the continuum. *Phys. Rev. A* **11**, 446–454 (1975).
179. Jain, A. & Shastry, C. Bound states in the continuum for separable nonlocal potentials. *Phys. Rev. A* **12**, 2237 (1975).
180. Molina, M. I., Miroshnichenko, A. E. & Kivshar, Y. S. Surface bound states in the continuum. *Phys. Rev. Lett.* **108**, 070401 (2012).
181. Gallo, N. & Molina, M. Bulk and surface bound states in the continuum. *J. Phys. A: Math. Theor.* **48**, 045302 (2015).
182. Simon, B. Some Schrödinger operators with dense point spectrum. *Proc. Amer. Math. Soc.* **125**, 203–208 (1997).
183. Moses, H. E. & Tuan, S. Potentials with zero scattering phase. *Il Nuovo Cimento* **13**, 197–206 (1959).
184. Gazdy, B. On the bound states in the continuum. *Phys. Lett. A* **61**, 89–90 (1977).
185. Meyer-Vernet, N. Strange bound states in the Schrödinger wave equation: when usual tunneling does not occur. *Am. J. Phys.* **50**, 354–356 (1982).
186. Pivovarchik, V. N., Suzko, A. A. & Zakhariev, B. N. New exactly solved models with bound states above the scattering threshold. *Phys. Scr.* **34**, 101 (1986).
187. Naboko, S. N. Dense point spectra of Schrödinger and Dirac operators. *Theor. Math. Phys.* **68**, 646–653 (1986).
188. Darboux, M. G. Sur une proposition relative aux équations liëaires. *C. R. Acad. Sci.* **94**, 1456–1459 (in French) (1882).
189. Svirsky, R. An application of double commutation to the addition of bound states to the spectrum of a Schrodinger operator. *Inverse Probl.* **8**, 483 (1992).
190. Pappademos, J., Sukhatme, U. & Pagnamenta, A. Bound states in the continuum from supersymmetric quantum mechanics. *Phys. Rev. A* **48**, 3525 (1993).
191. Stahlhofen, A. A. Completely transparent potentials for the Schrödinger equation. *Phys. Rev. A* **51**, 934–943 (1995).
192. Weber, T. A. & Pursey, D. L. Continuum bound states. *Phys. Rev. A* **50**, 4478–4487 (1994).
193. Kočinac, S. L. S. & Milanović, V. Bound states in continuum generated by point interaction and supersymmetric quantum mechanics. *Modern Phys. Lett. B* **26**, 1250177 (2012).
194. Ranjani, S. S., Kapoor, A. & Panigrahi, P. Normalizable states through deformation of Lamé and the associated Lamé potentials. *J. Phys. A Math. Theor.* **41**, 285302 (2008).
195. Prodanović, N., Milanović, V. & Radovanović, J. Photonic crystals with bound states in continuum and their realization by an advanced digital grading method. *J. Phys. A* **42**, 415304 (2009).
196. Petrović, J. S., Milanović, V. & Ikonić, Z. Bound states in continuum of complex potentials generated by supersymmetric quantum mechanics. *Phys. Lett. A* **300**, 595–602 (2002).
197. Andrianov, A. A. & Sokolov, A. V. Resolutions of identity for some non-Hermitian Hamiltonians. I. Exceptional point in continuous spectrum. *SIGMA* http://dx.doi.org/10.3842/SIGMA.2011.111 (2011).
198. Sokolov, A. V. Resolutions of identity for some non-Hermitian Hamiltonians. II. Proofs. *SIGMA* http://dx.doi.org/10.3842/SIGMA.2011.112 (2011).
199. Longhi, S. & Della Valle, G. Optical lattices with exceptional points in the continuum. *Phys. Rev. A* **89**, 052132 (2014).
200. Longhi, S. Bound states in the continuum in PT-symmetric optical lattices. *Opt. Lett.* **39**, 1697–1700 (2014).
This paper classifies and compares two types of BICs in parity-time symmetric systems.
201. Fernández-García, N., Hernández, E., Jáuregui, A. & Mondragón, A. Bound states at exceptional points in the continuum. *J. Phys. Conf. Ser.* **512**, 012023 (2014).
202. Garmon, S., Gianfreda, M. & Hatano, N. Bound states, scattering states, and resonant states in PT-symmetric open quantum systems. *Phys. Rev. A* **92**, 022125 (2015).
203. Demić, A., Milanović, V. & Radovanović, J. Bound states in the continuum generated by supersymmetric quantum mechanics and phase rigidity of the corresponding wavefunctions. *Phys. Lett. A* **379**, 2707–2714 (2015).
204. Correa, F., Jakubský, V. & Plyushchay, M. S. PT-symmetric invisible defects and confluent Darboux–Crum transformations. *Phys. Rev. A* **92**, 023839 (2015).
205. Pursey, D. & Weber, T. Scattering from a shifted von Neumann–Wigner potential. *Phys. Rev. A* **52**, 3932 (1995).
206. Weber, T. A. & Pursey, D. L. Scattering from a truncated von Neumann–Wigner potential. *Phys. Rev. A* **57**, 3534–3545 (1998).
207. Longhi, S. Non-Hermitian tight-binding network engineering. *Phys. Rev. A* **93**, 022102 (2016).
208. Corrielli, G., Della Valle, G., Crespi, A., Osellame, R. & Longhi, S. Observation of surface states with algebraic localization. *Phys. Rev. Lett.* **111**, 220403 (2013).
This work demonstrates a BIC in a tight-binding lattice with engineered hopping rates.
209. McIver, M. & Porter, R. Trapping of waves by a submerged elliptical torus. *J. Fluid Mech.* **456**, 277–293 (2002).
210. McIver, P. & Newman, J. N. Trapping structures in the three-dimensional water-wave problem. *J. Fluid Mech.* **484**, 283–301 (2003).
211. McIver, P. & McIver, M. Trapped modes in the water-wave problem for a freely floating structure. *J. Fluid Mech.* **558**, 53–67 (2006).
212. McIver, P. & McIver, M. Motion trapping structures in the three-dimensional water-wave problem. *J. Eng. Math.* **58**, 67–75 (2007).
213. Porter, R. & Evans, D. V. Water-wave trapping by floating circular cylinders. *J. Fluid Mech.* **633**, 311–325 (2009).
214. Meier, M. *et al.* Laser action from two-dimensional distributed feedback in photonic crystals. *Appl. Phys. Lett.* **74**, 7–9 (1999).
215. Imada, M. *et al.* Coherent two-dimensional lasing action in surface-emitting laser with triangular-lattice photonic crystal structure. *Appl. Phys. Lett.* **75**, 316–318 (1999).
216. Noda, S., Yokoyama, M., Imada, M., Chutinan, A. & Mochizuki, M. Polarization mode control of two-dimensional photonic crystal laser by unit cell structure design. *Science* **293**, 1123–1125 (2001).
217. Miyai, E. *et al.* Photonics: lasers producing tailored beams. *Nature* **441**, 946–946 (2006).
218. Matsubara, H. *et al.* GaN photonic-crystal surface-emitting laser at blue-violet wavelengths. *Science* **319**, 445–447 (2008).
219. Hirose, K. *et al.* Watt-class high-power, high-beam-quality photonic-crystal lasers. *Nat. Photonics* **8**, 406–411 (2014).
This paper shows continuous-wave lasing through a quasi-BIC with a high output-power and a low threshold at room temperature.

220. Yanik, A. A. *et al.* Seeing protein monolayers with naked eye through plasmonic Fano resonances. *Proc. Natl Acad. Sci. USA* **108**, 11784–11789 (2011).
221. Zhen, B. *et al.* Enabling enhanced emission and low-threshold lasing of organic molecules using special Fano resonances of macroscopic photonic crystals. *Proc. Natl Acad. Sci. USA* **110**, 13711–13716 (2013).
222. Foley, J. M., Young, S. M. & Phillips, J. D. Symmetry-protected mode coupling near normal incidence for narrow-band transmission filtering in a dielectric grating. *Phys. Rev. B* **89**, 165111 (2014).
223. Iwahashi, S. *et al.* Higher-order vector beams produced by photonic-crystal lasers. *Opt. Express* **19**, 11963–11968 (2011).
224. Kitamura, K., Sakai, K., Takayama, N., Nishimoto, M. & Noda, S. Focusing properties of vector vortex beams emitted by photonic-crystal lasers. *Opt. Lett.* **37**, 2421–2423 (2012).
225. Zhan, Q. Cylindrical vector beams: from mathematical concepts to applications. *Adv. Opt. Photonics* **1**, 1–57 (2009).
226. Fan, X. & White, I. M. Optofluidic microsystems for chemical and biological analysis. *Nat. Photonics* **5**, 591–597 (2011).
227. Morgan, D. *Surface Acoustic Wave Filters: With Applications to Electronic Communications and Signal Processing* Ch. 11 (Academic Press, 2007).
228. Benabid, F., Knight, J. C., Antonopoulos, G. & Russell, P. S. J. Stimulated raman scattering in hydrogen-filled hollow-core photonic crystal fiber. *Science* **298**, 399–402 (2002).
229. Couny, F., Benabid, F., Roberts, P. J., Light, P. S. & Raymer, M. G. Generation and photonic guidance of multi-octave optical-frequency combs. *Science* **318**, 1118–1121 (2007).
230. Benabid, F., Couny, F., Knight, J., Birks, T. & Russell, P. S. J. Compact, stable and efficient all-fibre gas cells using hollow-core photonic crystal fibres. *Nature* **434**, 488–491 (2005).
231. Dudley, J. M. & Taylor, J. R. Ten years of nonlinear optics in photonic crystal fibre. *Nat. Photonics* **3**, 85–90 (2009).
232. Benoît, A. *et al.* Over-five octaves wide Raman combs in high-power picosecond-laser pumped H_2-filled inhibited coupling Kagome fiber. *Opt. Express* **23**, 14002–14009 (2015).
233. Debord, B. *et al.* Hypocycloid-shaped hollow-core photonic crystal fiber part I: arc curvature effect on confinement loss. *Opt. Express* **21**, 28597–28608 (2013).
234. Mur-Petit, J. & Molina, R. A. Chiral bound states in the continuum. *Phys. Rev. B* **90**, 035434 (2014).
235. Zhang, J. M., Braak, D. & Kollar, M. Bound states in the continuum realized in the one-dimensional two-particle Hubbard model with an impurity. *Phys. Rev. Lett.* **109**, 116405 (2012).
236. Zhang, J. M., Braak, D. & Kollar, M. Bound states in the one-dimensional two-particle Hubbard model with an impurity. *Phys. Rev. A* **87**, 023613 (2013).
237. Longhi, S. & Della Valle, G. Tamm–Hubbard surface states in the continuum. *J. Phys. Condens. Matter* **25**, 235601 (2013).
238. Della Valle, G. & Longhi, S. Floquet–Hubbard bound states in the continuum. *Phys. Rev. B* **89**, 115118 (2014).
239. Vicencio, R. A. *et al.* Observation of localized states in Lieb photonic lattices. *Phys. Rev. Lett.* **114**, 245503 (2015).
240. Mukherjee, S. *et al.* Observation of a localized flat-band state in a photonic Lieb lattice. *Phys. Rev. Lett.* **114**, 245504 (2015).
241. Koirala, M. *et al.* Critical states embedded in the continuum. *New J. Phys.* **17**, 013003 (2015).
242. Joglekar, Y. N., Scott, D. D. & Saxena, A. PT-symmetry breaking with divergent potentials: lattice and continuum cases. *Phys. Rev. A* **90**, 032108 (2014).
243. Molina, M. I. & Kivshar, Y. S. Embedded states in the continuum for PT-symmetric systems. *Studies Appl. Math.* **133**, 337–350 (2014).
244. Longhi, S. Invisible surface defects in a tight-binding lattice. *Eur. Phys. J. B* **87**, 189 (2014).
245. Regensburger, A. *et al.* Observation of defect states in PT-Symmetric optical lattices. *Phys. Rev. Lett.* **110**, 223902 (2013).
This paper demonstrates a BIC in a pair of parity-time symmetric coupled fibre loops.
246. Capasso, F. *et al.* Observation of an electronic bound state above a potential well. *Nature* **358**, 565–567 (1992).
247. Albo, A., Fekete, D. & Bahir, G. Electronic bound states in the continuum above (Ga, In)(As, N)/(Al, Ga) As quantum wells. *Phys. Rev. B* **85**, 115307 (2012).
248. Bulgakov, E. N. & Sadreev, A. F. Robust bound state in the continuum in a nonlinear microcavity embedded in a photonic crystal waveguide. *Opt. Lett.* **39**, 5212–5215 (2014).
249. Bulgakov, E., Pichugin, K. & Sadreev, A. Channel dropping via bound states in the continuum in a system of two nonlinear cavities between two linear waveguides. *J. Phys. Condens. Matter* **25**, 395304 (2013).
250. Bulgakov, E. N., Pichugin, K. N. & Sadreev, A. F. All-optical light storage in bound states in the continuum and release by demand. *Opt. Express* **23**, 22520–22531 (2015).
251. Lannebere, S. & Silveirinha, M. G. Optical meta-atom for localization of light with quantized energy. *Nat. Commun.* **6**, 8766 (2015).
252. Pichugin, K. N. & Sadreev, A. F. Frequency comb generation by symmetry-protected bound state in the continuum. *J. Opt. Soc. Am. B* **32**, 1630–1636 (2015).
253. Crespi, A. *et al.* Particle statistics affects quantum decay and Fano interference. *Phys. Rev. Lett.* **114**, 090201 (2015).
254. Silveirinha, M. G. Trapping light in open plasmonic nanostructures. *Phys. Rev. A* **89**, 023813 (2014).
This paper proposes 3D confinement of light using an $\varepsilon = 0$ material and provides a non-existence theorem when $\varepsilon \neq 0$ (see BOX 1).
255. Monticone, F. & Alù, A. Embedded photonic eigenvalues in 3D nanostructures. *Phys. Rev. Lett.* **112**, 213903 (2014).
256. Hrebikova, I., Jelinek, L. & Silveirinha, M. G. Embedded energy state in an open semiconductor heterostructure. *Phys. Rev. B* **92**, 155303 (2015).
257. Mermin, N. D. The topological theory of defects in ordered media. *Rev. Mod. Phys.* **51**, 591 (1979).
258. Hasan, M. Z. & Kane, C. L. Colloquium: topological insulators. *Rev. Mod. Phys.* **82**, 3045 (2010).

Acknowledgements
The authors thank A. Maznev, N. Rivera, F. Wang, H. Zhou, M. Segev, N. Moiseyev, S. Longhi, P. McIver, M. McIver, F. Benabid, and S. G. Johnson for discussions. This work was partially supported by the National Science Foundation through grant no. DMR-1307632 and by the Army Research Office through the Institute for Soldier Nanotechnologies under contract no. W911NF-13-D-0001. B.Z., J.D.J. and M.S. were partially supported by S3TEC (analysis and reading of the manuscript), an Energy Frontier Research Center funded by the US Department of Energy under grant no. DE-SC0001299. B.Z. was partially supported by the United States–Israel Binational Science Foundation (BSF) under award no. 2013508.

Competing interests statement
The authors declare no competing interests.